Louisiana Water Resources Research Institute

Annual Technical Report

FY 2000

Introduction

This report presents a description of the activities of the Louisiana Water Resources Research Institute for the period of March 1, 2000 to February 28, 2001. The Louisiana Water Resources Research Institute (LWRRI) is unique among academic research institutions in the state because it is federally mandated to perform a statewide function of promoting research, education and services in water resources. The federal mandate recognizes the ubiquitous involvement of water in environmental and societal issues, and the need for a focal point for coordination.

As a member of the National Institutes of Water Resources, LWRRI is one of a network of 54 institutes nationwide initially authorized by Congress in 1964 and has been re-authorized through the Water Resources Research Act of 1984, as amended in 1996 by P.L. 104-147. Under the Act, the institutes are to: "1) plan, conduct, or otherwise arrange for competent research that fosters, (A) the entry of new research scientists into water resources fields, (B) the training and education of future water scientists, engineers, and technicians, (C) the preliminary exploration of new ideas that address water problems or expand understanding of water and water-related phenomena, and (D) the dissemination of research results to water managers and the public.

2) cooperate closely with other colleges and universities in the State that have demonstrated capabilities for research, information dissemination and graduate training in order to develop a statewide program designed to resolve State and regional water and related land problems. Each institute shall also cooperate closely with other institutes and organizations in the region to increase the effectiveness of the institutes and for the purpose of promoting regional coordination."

The National Water Resources Institutes program establishes a broad mandate to pursue a comprehensive approach to water resource issues that are related to state and regional needs. Louisiana is the water state; no other state has so much of its cultural and economic life involved with water resource issues. The oil and gas industry, the chemical industry, port activities, tourism and fisheries are all dependent upon the existence of a deltaic landscape containing major rivers, extensive wetlands, numerous large shallow water bays, and large thick sequences of river sediments all adjacent to the Gulf of Mexico. Finally, many of the problems facing the state are derived from changes taking place in or affecting this delta landscape, including coastal erosion, landloss, sea level rise and climate change, hurricane flooding, run-off and riverine flooding, degradation of water quality and hypoxia.

The Institute is administratively housed in the College of Engineering and maintains working relationships with several research and teaching units at Louisiana State University. Recent cooperative research projects have been conducted with Center for Coastal, Energy, & Environmental Resources, the Louisiana Geologic Survey and the Colleges of Basic Sciences, the College of Arts and Sciences, and the Hurricane Center.

Research Program

RESEARCH

The research program of the Louisiana Water Resources Research Institute is concentrated on addressing a few core issues that form the basis for satisfying the immediate needs of the state and for expanding the program in the future. These issues include small watershed hydrology, coastal flooding, non-point source pollution, and hydrologic modeling. The research program has two components. One component is the research being conducted by Institute staff supported by external funding. The other is component is the contract research funded by the Institute from the USGS grant.

The approach being pursued in the research program is; 1. Focus the technology base of the program on advanced technology and high-end computing. This means working with new data collection techniques such as LIDAR for mapping small watershed topography. It also means developing distributed computing capability, i.e., clusters of computers, to process and GIS software to visualize extremely large data sets. Finally it means the development and use of complex integrated environmental and infrastructure computer models. 2. Address the immediate needs of the state in the areas of flood control, coastal restoration, and non-point source pollution. 3. Maintain a working relationship with the state USGS office, and with state and federal governmental agencies. 4. Become directly involved with the public through education and assistance programs. 5. Identify and develop new opportunities for program growth in regional, national an international issues.

EXTERNALLY FUNDED RESEARCH

The externally funded research in the Institute is conducted within the Natural Systems Engineering Laboratory. Current projects include: 1. Climatology and Hydrology of the Upper Pontchartrain Basin, for the Lake Pontchartrain Basin Foundation. 2. Technical Assistance for Complex Project Development, for the Coastal Wetland Protection, Planning and Restoration Act. 3. Hurricane Shelter Assessment and Flooding, for St. James Parish. 4. Completion of the Lower Atchafalaya Reevaluation for the New Orleans District, U. S. Army Corps of Engineers. 5. Flood Damage Prevention Using Remotely Sensed Data and a Mesoscale Atmospheric Model, for the National Aeronautics and Space administration. The total funding associated with these projects is $ 385,000.

BASE GRANT RESEARCH

The 2000 contract research program of the Louisiana Water Resources Research Institute addressed several priority water resources problem areas identified for Louisiana; flooding, wetland wastewater treatment, and urban nonpoint sources of pollution. Three research projects were completed during the current year: (1) Investigations into the Effect of the Direction, Spatial Coverage and Temporal Distribution of Rainfall on Watershed Flooding; (2) Denitrification in Wetlands Receiving Mississippi River Freshwater Diversion: Water Quality Aspects; and (3) Quantifying Urban Non-point Sources of Lead for use in TMDL Computations. These projects address important in Louisiana with it's vast wetland areas, agricultural base, and threatened ecosystems. The final reports for each of these projects follows.

Basic Information

Title:	Investigations into the Effect of the Direction, Spatial Coverage and Temporal Distribution of Rainfall on Watershed Flooding
Project Number:	GR02673 C-02 FY00
Start Date:	3/1/2000
End Date:	2/28/2001
Research Category:	Climate and Hydrologic Processes
Focus Category:	Floods, Hydrology, Surface Water
Descriptors:	Drainage, flooding, rainfall, rainfall-runoff models, watershed modeling, and urban hydrology
Lead Institute:	Louisiana Water Resources Research Institute
Principal Investigators:	Vijay Singh

Publication

EFFECT OF THE DURATION AND DIRECTION OF STORM MOVEMENT ON PLANAR FLOW WITH FULL AND PARTIAL AREAL COVERAGE

Vijay P. Singh
Department of Civil and Environmental Engineering
Louisiana State University
Baton Rouge, LA 70780-6405

Abstract: Using kinematic wave equations analytical solutions are derived for flow due to storms moving either up or down the plane and covering it fully or partially. By comparing the flow due to a moving storm with that due to a stationary storm of the same duration and areal coverage, the influence of storm duration, direction ans areal coverage is investigated. It is found that the direction, duration, and areal coverage of storm movement have a pronounced effect on the discharge hydrograph.

1. INTRODUCTION

The importance of storm movement on surface runoff has been investigated for nearly four decades. Singh (1997) presented a survey of investigations dealing with the influence of storm movement. There are three aspects of storm movement for quantifying its influence of on the discharge hydrograph: (1) direction (e.g., upstream, downstream, transverse, or angular), (2) areal coverage (e.g., full or partial), and (3) duration (e.g., duration leading to equilibrium hydrograph or partial equilibrium hydrograph). In a previous paper, Singh (1998) investigated the effect of the direction of storm movement on planar flow. However, in that study as well as in others surveyed previously, the usual assumption is that when storm rainfall occurs, it covers the entire watershed even though it may not be true in reality.

Maksimov (1964) showed that the rainstorm movement altered peak discharge. Marcus (1964) experimentally showed the importance of the rainstorm movement to the time distribution of surface runoff. Roberts and Klingman (1970) found that the direction of storm movement might augment or reduce flood peaks and modify the hydrograph recession. Surkan (1974) observed that peak flow rates and average flow rates were most sensitive to changes in the direction and speed of the rainstorms. Niemczynowicz (1984a,b) determined the influence of storm direction, intensity,

velocity, and duration on the runoff hydrograph and peak discharge on a conceptual watershed and a real watershed in the City of Lund in Sweden

Yen and Chow (1968) experimentally investigated surface runoff due to moving rainstorms. Sargent (1981, 1982) determined the effects of storm direction and speed on peak runoff, flood volume, and hydrograph shape. Stephenson (1984) simulated runoff hydrographs from a storm travelling down a watershed. Jenson (1984) determined the influence of storm movement and its direction on the shape, peak, time to peak and other characteristics of the runoff hydrograph. Foroud et al. (1984) employed a 50-year hypothetical moving rainstorm to quantify the effect of its speed and direction on the runoff hydrograph. Ngirane-Katashaya and Wheater (1985) analyzed the effect of storm velocity on runoff hydrograph. Ogden et al. (1995) investigated the influence of storm movement on runoff. Singh (1998) examined the effect of the direction of storm movement on planar flow.

Employing the kinematic wave theory, this paper examines the influence on planar flow of storms which may move up or down a plane and cover it fully or partially. It is well known that when a rainstorm occurs, it may occur over only a portion of the watershed. An analytical treatment of the effect of storm direction and duration occurring over portion of the watershed does not appear to have been reported in the literature. Most of the studies reported in the literature have either been numerical or empirical. Analytical solutions provide considerable insight into the relation between storm dynamics and flow dynamics. By comparing the flow due to a moving storm with that due to a stationary storm of the same duration it investigates the influence of storm direction, duration and areal coverage on the flow hydrograph.

2. PLANAR FLOW: STORM MOVEMENT DOWNSTREAM WITH FULL AREAL COVERAGE

Consider a storm occurring over a plane of length L, width unity (W=1), and slope S_o in the downstream direction. It is assumed that the storm occurs for a certain duration which is sufficiently long to cover the entire plane. Let this duration be equal to T. However, this duration of storm occurrence is not the same everywhere on the pane. At the head of the plane, this duration is actually T but decreases downstream in proportion to the time taken by the storm which is directly proportional to the storm velocity. In a previous paper, Singh (1998) assumed the duration T of storm

occurrence to be the same everywhere on the plane. Thus, the treatment in what follows is fundamentally different. Let the storm rainfall of intensity q cover the plane length of L. It is assumed that the storm moves with a constant velocity V_S. The storm travel path is then given by $t = x/V_S$. At any location x on the plane, rainfall q lasts for the duration equal to

$$T(x) = t - \frac{x}{V_S} \tag{1}$$

It is assumed that infiltration is either included in q or neglected. The flow continuity equation can be expressed as

$$\frac{\partial h}{\partial t} + \frac{\partial Q}{\partial x} = q\,(x, \zeta) \tag{2}$$

and the kinematic wave equation can be written as

$$Q = uh = \alpha h^{\,n} \tag{3}$$

where $\zeta = t - x/V_S$ and defines the duration for which the storm has occurred at any time at the position x. Here the time taken by the storm to cover the plane is defined by L/V_S. Thus, the occurrence of the storm can be expressed as

$$q = 0\,, \tau \leq 0\,;\; q > 0\,; \zeta > 0\,; q = 0, t > T \tag{4}$$

Substitution of equation (3) in equation (2) yields

$$\frac{\partial h}{\partial t} + n\alpha h^{n-1}\frac{\partial h}{\partial x} = q(x, \tau) \tag{5}$$

To solve equation (5) the initial (IC) and boundary (BC) conditions are taken as

3

$$IC: \quad h(x, \frac{x}{V_S}) = 0 \tag{6}$$

$$BC: \quad h(0, t) = 0 \tag{7}$$

Solution of equation (5), subject to equations (6) and (7), can be derived using the method of characteristics (see Singh 1996 for a complete treatment). With t as the characteristic parameter, the characteristic form of equation (5) is

$$\frac{dh}{dt} = q(x, \zeta) \tag{8}$$

$$\frac{dx}{dt} = n\alpha h^{n-1} \tag{9}$$

It is, however, more convenient to choose x as the characteristic parameter and write equations (8) and (9) as

$$\frac{dh}{dx} = \frac{q(x, \tau)}{n\alpha h^{n-1}} \tag{10}$$

$$\frac{dt}{dx} = \frac{1}{n\alpha h^{n-1}} \tag{11}$$

The problem of planar flow is formulated in equations (10) and (11) subject to equations (6) and (7).

4

For evolution of runoff due to a given storm two possibilities exist: (1) The storm duration T is long and the resulting hydrograph is an equlibrium hydrograph. The solution domain for this case is shown in Figure 1. The solution domain, shown in Figure 1, is comprised of domains D_1, D_2, and D_3. Domain D_1 is bounded by $x = 0$, $t = x/V_S$, $0 \le x \le L$, $x = L$, and $t(x,0)$; domain D_2 by $x=0$, $t = t (x,0)$, $x = L$, and $t = T$; and D_3 by $t = T$, $x=0$, and $x = L$. (2) The storm duration T is not long enough and the resulting hydrograph is a partial equilibrium hydrograph. The solution domain for this case is shown in Figure 2. The solution domain, shown in Figure 2, is comprised of domains D_1, D_2, D_{3A}, and D_{3B}. Domain D_1 is bounded by $x = 0$, $x = L$, $t = x/V_S$; domain D_2 by $x = 0$, $t = T$, and $t = t (x, 0)$; domain D_{3A} by $t = T$, $x = 0$, $t = t(x, \bar{x})$, and $x = L$; and domain D_{3B} by $x = L$, $t = t(x, \bar{x})$, and $t = T$.

2.1 Equilibrium Hydrograph

The solution in each domain is derived in what follows.

2.1.1 Domain D_1: Let x_0, $0 \le x_0 \le L$, be a parameter denoting the intersection of a characteristic curve with the curve $t=x/V_S$; indeed the characteristics issue from this curve. The initial condition given by equation (6) is expressed in parametric form

$$h(x_0, \frac{x_0}{V_S}) = 0 \qquad (12)$$

Equations (10) and (11) constitute a coupled system and hence equation (10) is solved first. Its solution is inserted in equation (11) which then is solved next. Solution of equation (10), subject to equation (12), follows

$$h = \left(\frac{q}{\alpha}\right)^{1/n} (x - x_0)^{1/n} \qquad (13a)$$

Solution of equation (11) is

$$t = \frac{x_0}{V_S} + q^{-\frac{(n-1)}{n}} \left(\frac{x - x_0}{\alpha}\right)^{1/n} \qquad (13b)$$

It should be renoted that $0 \le x_0 \le L$. Eliminating x_0 between equations (13a) and (13b) one gets an inverted expression for h has as a function of x and t.

$$t = \frac{x_0}{V_s} + \frac{h}{q} - \frac{\alpha h^n}{q V_s} \qquad (14a)$$

Recalling the definition of flow velocity, $V_f = \alpha h^{(n-1)}$, equation (14a) can be expressed as

$$h(x,t) = \frac{q}{V_s - V_f} (t V_s - x) \qquad (14b)$$

The discharge is given by

$$Q(x,t) = \alpha h^n = h V_f = \frac{V_f}{V_s - V_f} q (t V_s - x) \qquad (14c)$$

It is noted that the flow depth depends on both x and t, i.e., the flow is both unsteady and nonuniform. Were the storm not moving, the flow would be unsteady but uniform. Thus the effect of storm movement on the rising hydrograph is apparent.

2.1.2 Domain D$_2$: Let t_0, $0 \le t_0 \le T$, be a parameter denoting the intersection of a characteristic with the line x=0; the characteristics t(x,t$_0$) issue from this line. The boundary condition, given by equation (7), is expressed in parametric form as

$$h(0, t_0) = 0 \qquad (15)$$

The solution of equations (10) and (11), subject to equation (15), is

$$h = \left(\frac{qx}{\alpha} \right)^{1/n} \qquad (16a)$$

6

Equations (16) and (17) are uncoupled and show that the flow depth is steady but nonuniform.

$$t = t_0 + q^{-\frac{(n-1)}{n}} \left(\frac{x}{\alpha} \right)^{1/n} \tag{16b}$$

$$h(x,t) = \left(\frac{qx}{\alpha} \right)^{1/n} \tag{17a}$$

Therefore, the flow depth, as a function of space and time, can be expressed as
and the discharge as

$$Q(x,t) = q\,x \tag{17b}$$

In this domain the storm movement has no influence on the flow hydrograph.

2.1.3 Domain D$_3$: Let x_0^*, $0 \le x_0^* \le L$, be a parameter denoting the intersection of a characteristic with $t = T$. The initial condition for this domain is supplied by the solution in domain D$_2$. We can write this condition as

$$h = \left(\frac{qx_0^*}{\alpha} \right)^{1/n} \tag{18}$$

The connection between t_0 and x_0^* can be expressed as

$$T = t_0 + q^{-\frac{(n-1)}{n}} \left(\frac{x_0^*}{\alpha} \right)^{1/n} \tag{19}$$

In domain D$_3$, the solution of equations (10) and (11), subject to equation (18), is

7

$$h(x,x_0^*) = \left(\frac{qx_0^*}{\alpha}\right)^{1/n} \qquad (20)$$

$$t_0 = T - q^{-\frac{(n-1)}{n}}\left(\frac{x_0^*}{\alpha}\right)^{1/n} \qquad (21)$$

Equations (21) and (22) constitute a parametric solution in domain D_3. Eliminating x_0^* between them one obtains

$$t = T + \frac{1}{n\,\alpha}\left(\frac{qx_0^*}{\alpha}\right)^{-\frac{(n-1)}{n}}(x-x_0^*) \qquad (22)$$

$$t = T + \frac{x}{n\,\alpha\,h^{n-1}} - \frac{h}{nq} \qquad (23)$$

Equation (23) shows the dependence of flow depth on x and t, i.e., the flow is both unsteady and nonuniform.

2.2 Partial Equilibrium Hydrograph

The solution in each domain is given in what follows.

2.2.1 Domain D$_1$: The solution in this domain is the same as before and is given by equations (13)-(14).

2.2.2 Domain D$_2$: The solution in this domain is the same as before and is given by equations (15)-(17).

2.2.3 Domain D$_{3A}$: The solution in this domain is the same as in Domain D_3 above, except that x_0^* varies between 0 and $\bar{x}$, and is given by equations (18)-(23).

8

2.2.4 <u>Domain D_{3B}</u>: Let the parameter be x_0^*, $\bar{x} \le x_0^* \le L$, denoting the intersection of a characteristic with the line $t=T$. The initial condition for domain D_{3B} is given by the solution in domain D_1 as

$$h = \left(\frac{q}{\alpha}\right)^{1/n} (x_0^* - x_0)^{1/n} \tag{24}$$

The connection between x_0 and x_0^* is given by

$$T = \frac{x_0}{V_S} + q^{-\frac{(n-1)}{n}} \left(\frac{x_0^* - x_0}{\alpha}\right)^{1/n} \tag{25}$$

From equation (25), knowing x_0 the other parameter x_0^* can be obtained. The solution in this

$$h(x, x_0^*) = \left(\frac{q}{\alpha}(x_0^* - x_0)\right)^{1/n}, \quad \bar{x} \le x_0^* \le L \tag{26}$$

domain, subject to equation (24), follows:

Equations (26) and (27) constitute the parametric solution in domain D_{3B}. The flow depth is both unsteady and nonuniform and reflects the influence of storm movement and its duration.

3. PLANAR FLOW: STORM MOVEMENT UPSTREAM WITH FULL AREAL

$$t(x, x_0^*) = T + \frac{1}{n\alpha} \left[\frac{q}{\alpha}(x_0^* - x_0)\right]^{-\frac{(n-1)}{n}} (x - x_0^*) \tag{27}$$

COVERAGE

The storm is moving in the upstream direction at a velocity of V_s. The storm follows the path defined by $t=(L-x)/V_s$. Depending on the duration of the storm T, two cases are distinguished. In the first case, T is sufficiently long such that the resulting hydrograph is an equilibrium hydrograph. The solution domain for this case is shown in Figure 3 and is partitioned in 3 subdomains D_1, D_2 and D_3. Domain D_1 is bounded by x=L, $t = t(x, L/V_S)$, and $t=(L-x)/V_S$; domain

9

D_2 is bounded by x = 0, t=(x, L/V_s), t = T, x = L; and domain D_3 is bounded by t = T, x = L, and x = 0. In the second case, T is short such that the resulting hydrograph is a partial equlibrium hydrograph. The solution domain for this case is sketched in Figure 4 and is divided into Domains D_1, D_2, D_{3A}, and D_{3B}. Domain D_1 is bounded by x = L, t = T, t = t (x, L/V_S), and t=(L-x)/V_S; domain D_2 is bounded by x = 0, t = T, and t = t (x, L/V_S); domain D_{3A} is bounded by t = T, t = t (x, $\bar{x}$), and x = L; and domain D_{3B} is bounded by x=L, t = t(x, $\bar{x}$), and x = L.

In the case of storms moving upstream, the duration for which the storm has lasted at any t at position x is given by

$$\zeta = t - \frac{L-x}{V_S} \tag{28}$$

The initial and boundary conditions, respectively, are

$$h(x, \frac{L-x}{V_S}) = 0 \tag{29}$$

$$h(0,t) = 0 \tag{30}$$

3.1 Equilibrium Hydrograph

The solution in each domain of this case is derived following the same procedure as for the storms moving downstream.

3.1.1 Domain D_1 **:** Let there be a parameter x_0 denoting the intersection of a characteristic with the curve t=(L-x)/V_S, $0 \leq x_0 \leq L$. The initial condition, given by equation (29), is expressed in

$$h(x_0, \frac{L-x_0}{V_S}) = 0 \tag{31}$$

parametric form as

10

Solution of equations (10) and (11), subject to equation (31), follows:

$$h(x, x_0) = \left(\frac{q}{\alpha}\right)^{1/n} (x - x_0)^{1/n} \tag{32}$$

$$t(x, x_0) = \frac{L - x_0}{V_S} + q^{-\frac{(n-1)}{n}} \left(\frac{x - x_0}{\alpha}\right)^{1/n}, \quad 0 \le x_0 \le L \tag{33}$$

3.1.2 <u>Domain D_2</u> : The boundary condition is given as

$$h\,(0,\, t_0\,) = 0,\; t_0 \ge L/V_S \tag{34}$$

The solution of equations (10) and (11), subject to equation (34), is given as

$$h = \left(\frac{qx}{\alpha}\right)^{1/n} \tag{35}$$

$$t = t_0 + q^{-\frac{(n-1)}{n}} \left(\frac{x}{\alpha}\right)^{1/n} \quad, \frac{L}{V_S} \le t_0 \le T \tag{36}$$

Equations (35) and (36) are uncoupled and show that the flow depth is steady but nonuniform. Therefore, the flow depth as a function of space and time can be expressed as

$$h(x, t) = \left(\frac{qx}{\alpha}\right)^{1/n} \tag{37}$$

and the discharge as

11

$$Q(x,t) = q\,x \tag{38}$$

In this domain the storm movement has no influence on the flow hydrograph.

3.1.3 <u>Domain D_3</u> : The initial condition is given as

$$h(x_0^*, T) = \left(\frac{q\,x_0^*}{\alpha}\right)^{1/n} \tag{39}$$

The solution of equations (10) and (11), subject to equation (39), is given as

$$h(x, x_0^*) \;=\; h(x_0) \;=\; h_0 \;=\; \left(\frac{q\,x_0^*}{\alpha}\right)^{\frac{1}{n}} \tag{40}$$

$$t(x, x_0^*) = T + \frac{x - x_0^*}{n\,\alpha\,h_0^{\,n-1}} \tag{41}$$

The connection between x_0^* and t_0 is given by equation (36) as

$$T \;=\; t_0 \;+\; q^{-\frac{(n-1)}{n}}\,\left(\frac{x_0^*}{\alpha}\right)^{\frac{1}{n}}, \qquad \frac{L}{V_S} \le t_0 \le T \tag{42}$$

This shows that the storm duration as well as the direction influence the runoff hydrograph.

3.2 Partial Equilibrium Hydrograph

The solution in each domain is given in what follows.

3.2.1 <u>Domain D_1</u> : The solution is given by equations (32) and (33).

3.2.2 <u>Domain D_2</u> : The solution is given by equations (35) and (36).

3.2.3 <u>Domain D_{3A}</u> : The solution is given by equations (40) and (41). Here $0 \le x_0^* \le \bar{x}$.

12

3.2.4 <u>Domain</u> $_{3B}$: Here $\bar{x} \le x_0^* \le L$. The value of $\bar{x}$ can be determined as follows:

$$T - \frac{L}{V_S} - q^{-\frac{(n-1)}{n}} \left(\frac{\bar{x}}{\alpha} \right)^{1/n} = 0 \tag{42}$$

Equation (42) can be solved for $\bar{x}$. In this domain the characteristic parameter is x_0^*, $\bar{x} \le x_0^* \le L$. The initial condition is given by the solution of domain D_1 :

$$h(x_0^*, x_0) = \left(\frac{q(x_0^* - x_0)}{\alpha} \right)^{1/n} \tag{43}$$

Solution of equations (10) and (11) with q=0, subject to equation (43), follows:

$$h(x, x_0^*) = \left[\frac{q(x_0^* - x_0)}{\alpha} \right]^{1/n} \tag{44}$$

$$t(x_0, x_0^*) = T + q^{-\frac{(n-1)}{n}} (\frac{x_0^* - x_0}{\alpha})^{-\frac{(n-1)}{n}} (x - x_0^*) \tag{45}$$

Equations (43) - (45) constitute the parametric solution in terms of h as a function of space and time in domain D_{3B}, and show the dependence of h on both x and t, i.e., the flow is both unsteady and nonuniform.

4. PLANAR FLOW: STORM MOVEMENT DOWNSTREAM WITH PARTIAL COVERAGE

The storms may move up or down a plane but may not fully cover it. Partial coverage of the plane by the storm means that the storm duration is limited and not large enough to cover the entire plane. It is well known that when a rainstorm occurs, it may occur only over a portion of the watershed. This is true whether the storm is moving or stationary. We consider a plane of length L

13

and width unity. It is assumed that the storm does not occur for a sufficiently long duration and

$$T(x) = \frac{aL}{V_S} - \frac{x}{V_S} \quad , \quad 0 \le x \le a\,L \tag{46}$$

hence does not cover the entire plane. Let the storm cover the plane length of al where a, $0 \le a \le 1$, is a fraction, Thus, there is a region (1-a) L not covered by the storm. In other words, the region 0 $\le$ x $\le$ aL is covered by the storm and the region aL$\le$x$\le$L is not covered by the storm. We first examine the case when the storm direction is downstream. At any location x on the plane, rainfall q lasts for the duration equal to where T(x) defines the time for which the storm has occurred at the position x; and V_S is the storm velocity. At x = 0, the duration of storm T is defined as L/V_S. It is assumed that infiltration is either not included or is a part of q.

The flow continuity equation is given by equation (2) and the kinematic wave equation by equation (3) in which $\zeta = t - x/V_S$ and defines the duration for which the storm has occurred at the position x and at time t. Thus, the occurrence of the storm can be expressed as

$$q = 0\,,\tau \le 0\,;\; q > 0\,;\zeta > 0\,;\, q = 0,\tau > \frac{a\,L - x}{V_S} \tag{47}$$

To solve equations (2) and (3), the initial (IC) and boundary (BC) conditions are taken as specified by equations (6) and (7). Thus, the problem of planar flow is formulated in equations (10) and (11) or equations (46) and (47) subject to equations (6) and (7). The solution domain for this case is shown in Figure 11 and is comprised of domains D_1, D_2, D_{3A} D_{3B}, D_{4A}, and D_{4B}. Domain D_1 is bounded by t = x/V_S, $0 \le$ x $\le$ a L, x = aL, t = aL/V_S and t(x,0); domain D_2 is bounded by x=0, 0 $\le$ t $\le$ a L/V_S, t = aL/V_S, and t = t (x,0); and D_{3A} is bounded by t = aL/V_S, x=0, t =t(x, $\bar{x}$), and x = aL; D_{3B} by t = aL/V_S, x = aL, and t (x, $\bar{x}$); domain D_{4A} is bounded by x = aL, x = L, t $\ge$(x, $\bar{s_0}$); domain D_{4B} is bounded by t = t(x, aL), x = aL, x = L, and t $\le$(x, $\bar{s_0}$).

14

4.1 Domain D_1

Let x_0, $0 \le x_0 \le aL$, be a parameter denoting the intersection of a characteristic curve with the curve $t = x/V_S$; indeed the characteristics issue from this curve. Solution for this domain is given by equation (13a) and (13b) or equation (14a) and (14b). The discharge is given by equation (14c). It is noted that the flow depth depends on both x and t, i.e., the flow is both unsteady and nonuniform. Were the storm not moving, the flow would be unsteady but uniform. Thus, the effect of storm movement on the rising hydrograph is apparent.

4.2 Domain D_2

Let t_0, $0 \le t_0 \le aL/V_S$, be a parameter denoting the intersection of a characteristic with the line x=0; the characteristics $t(x,t_0)$ issue from this line. The solution for this domain is given by equations (16a) and (16b), or equations (17a) and (17b). In this domain the storm movement has no influence on the flow hydrograph.

4.3 Domain D_{3A}

Let x_0^*, $0 \le x_0^* \le \bar{x}$, be a parameter denoting the intersection of a characteristic with $t = aL/V_S$. The initial condition for this domain is supplied by the solution in domain D_2. The connection between t_0 and x_0^* can be expressed as

$$\frac{aL}{V_S} = t_0 + q^{-\frac{(n-1)}{n}} \left(\frac{x_0^*}{\alpha} \right)^{1/n} \tag{48}$$

In domain D_{3A}, the solution in parametric form is given by equation (20) and

$$t = \frac{aL}{V_S} + \frac{1}{n\,\alpha} \left(\frac{q\,x_0^*}{\alpha} \right)^{1/n} (x - x_0^*) \tag{49}$$

Eliminating x_0^* between them one obtains

15

$$t = \frac{aL}{V_S} + \frac{x}{n\alpha h^{n-1}} - \frac{h}{nq} \tag{50}$$

Equation (50) shows the dependence of flow depth on x and t, i.e., the flow is both unsteady and nonuniform. It also shows the extent of partial coverage of the plane by the storm.

4.4 Domain D_{3B}

Let the parameter be x_0^*, $\bar{x} \leq x_0^* \leq aL$, denoting the intersection of a characteristic with the line $t=T=aL/V_S$. The initial condition for domain D_{3B} is given by the solution in domain D_1 in equation (24). The connection between x_0 and x_0^* is given by

$$\frac{aL}{V_S} = \frac{x_0}{V_S} + q^{-\frac{(n-1)}{n}} \left(\frac{x_0^* - x_0}{\alpha} \right)^{1/n} \tag{51}$$

The solution in parametric form in this domain is given by equation (26) and

$$t(x,x_0^*) = \frac{aL}{V_S} + \frac{1}{n\alpha} \left[\frac{q}{\alpha}(x_0^* - x_0) \right]^{-\frac{(n-1)}{n}} (x - x_0^*) \tag{52}$$

The flow depth is both unsteady and nonuniform and reflects the influence of storm movement and its duration.

4.5 Domain D_{4B}

Now consider the region not covered by the storm, i.e., $a = aL$ to $x = L$. The characteristics originating from the line $x = aL$ after $t = aL/V_S$ will elongate to the line $x = L$, and these characteristics are of domain D_{3B}. Let s_0 be the parameter denoting the intersection of a characteristic with the time segment $T \leq t \leq s_0$, where s_0 is the point where the bounding characteristic $t = t(x, \bar{x})$ intersects the line $x = aL$. Clearly, s_0 satisfies $aL/V_S \leq s_0 \leq \bar{s}_0$. The characteristic solution in parametric form is given by equation (26) and

16

$$t(x, s_0) = s_0 + \frac{1}{n\,\alpha\,h_0^{n-1}}(x - aL) \tag{53}$$

where

$$s_0 = \frac{aL}{V_s} + \frac{1}{n\alpha}\left[\frac{q}{\alpha}(x_0^* - x_0)\right]^{-(n-1)/n}(aL - x_0^*) \tag{54}$$

and

$$\overline{s_0} = \frac{aL}{V_s} + \frac{1}{n\alpha}\left[\frac{q\,\overline{x}}{\alpha}\right]^{-(n-1)/n}(aL - \overline{x}) \tag{55}$$

The solution shows the dependence of flow depth on x and t, indicating that the flow is both unsteady and nonuniform. It also reflects the influence of the extent of the coverage of the plane by the storm.

4.7 Domain D_{4A}

In this domain, $s_0 \geq \overline{s_0}$. The characteristic solution is given by

$$h(x,s_0) = h_0 = \left(\frac{q x_0^*}{\alpha}\right)^{1/n} \tag{56a}$$

$$t(x,s_0) = s_0 + \frac{1}{n\alpha h_0^{n-1}}(x - aL) \tag{56b}$$

17

where x_0^* and s_0 are related as

$$s_0 = \frac{aL}{V_s} + \frac{1}{n\alpha}\left[\frac{q\,x_0^*}{\alpha}\right]^{\frac{(1-n)}{n}}(aL - x_0^*)$$ (57)

The solution shows the dependence of the flow depth on both x and t, and the extent of the coverage of the plane by the storm. The flow is both unsteady and nonuniform.

5. PLANAR FLOW: STORM MOVEMENT UPSTREAM WITH PARTIAL AREAL COVERAGE

The storm is moving in the upstream direction at a velocity of V_s. The storm follows the path defined by $t=(L-x)/V_s$. The solution domain for this case is shown in Figure 12 and is partitioned in 3 subdomains D_{1A}, D_{1B} and D_3. Domain D_{1A} is bounded by x=L, t = t(x, $\bar{x}$), and t = (L-x)/V_S), $\bar{x}$ ≤x ≤ L; domain D_{1B} is bounded by t=(L-x)/V_s), aL ≤x ≤ $\bar{x}$, t = t(x, $\bar{x}$), and t = (1-a) L/ V_S ; and domain D_3 is bounded by t = (1-a)L/V_S, x = aL, and x = L. The solution in these domains is derived following the same procedure as before. In the case of storm moving upstream the duration for which the storm lasts at any position is given as

$$T(x) = \frac{(1-a)L}{V_s} - \frac{L-x}{V_s} = \frac{x-a\,L}{V_s}$$ (58)

The initial and boundary conditions are given by equations (29) and

$$h(aL,t) = 0$$ (59)

5.1 Domain D_{1A}

Let there be a parameter x_0 denoting the intersection of a characteristic with the curve t=(L-x)/V_S, aL ≤ x_0 ≤ $\bar{x}$. Solution for this domain is given by equation (32) and (33). The value of $\bar{x}$

18

can be determined as

$$\frac{aL}{V_S} - \frac{\bar{x}}{V_S} + q^{-(n-1)/n} \left(\frac{L-\bar{x}}{\alpha}\right)^{1/n} = 0 \tag{60}$$

The flow in this domain is both unsteady and nonuniform. The effect of storm direction and partial coverage is apparent.

5.2 Domain D_{1B}

The solution in this domain is the same as in domain D_{1A} except that $0 \le x_0 \le \bar{x}$.

5.3 Domain D_3

In this domain the characteristic parameter is x_0^*, $aL \le x_0^* \le L$. The initial condition is given by equation (43). The solution for this domain is given by equation (43) and

$$t(x_0, x_0^*) = \frac{(1-a)L}{V_S} + \frac{L-x_0}{V_S} + q^{-\frac{(n-1)}{n}} \left(\frac{x_0^* - x_0}{\alpha}\right)^{\frac{1}{n}} \tag{61}$$

or

$$t(x, x_0^*) = \frac{(1-a)L}{V_S} + \frac{1}{n\alpha} \left[\frac{q}{\alpha}(x_0^* - x_0)\right]^{\frac{(1-n)}{n}} (x - x_0^*) \tag{62}$$

Equations (43) and (61) constitute a parametric solution and show the dependence of of h on both x and t, i.e., the flow depth is both unsteady and nonuniform.

6. APPLICATION FOR STORMS COVERING THE ENTIRE PLANE

The effect of the direction and duration of storm movement on planar flow was analyzed considering both moving and stationary storms. The storm velocities were taken as 1.5 and 10 times

19

the normalizing velocity of flow.. Depending on the duration of the storm the hydrograph at the downstream end of the plane would be either an equilibrium or partially equilibrium hydrograph.

For purposes of comparison and ease of graphical portrayal it is more convenient to employ dimensionless solutions. To that end the following normalizing quantities were defined:

$$U = \text{normalizing flow velocity} = \alpha H_0^{n-1} \tag{63}$$

$H_0 = $ normalizing flow depth

$L = $ normalizing distance = plane length

$T = $ normalizing time which is the same as the equilibrium time defined below.

$$D = \text{time to equilibrium} = \text{time of concentration } (t_c) = L / U \tag{64}$$

$$Q_0 = \text{normalizing discharge} = \alpha H_0^n = H_0 U = q_{max} L \tag{65}$$

$$q_{max} = \text{maximum rainfall intensity} = H_0/D = \frac{U H_0}{L} = \frac{Q_0}{L} \tag{66}$$

The normalizing quantities were in accord with a stationary storm. Thus, the dimensionless quantities can be defined as

$$\zeta^* = \frac{t}{D} - \frac{xU}{V_s L}, V_s^* = \frac{V_s}{U}, T_* = \frac{T}{D} \quad x^* = \frac{x}{L}, t^* = \frac{t}{D} = \frac{tU}{L}, h^* = \frac{h}{H_0}, Q^* = \frac{Q}{Q_0} = \frac{Q}{L q_{max}}, q^* = \frac{q}{q_{max}}$$

$$\tag{67}$$

Using these quantities dimensional solutions were rendered dimensionless. Appendix A contains dimensionless solutions.

6.1 Stationary Storms Covering the Entire Plane

Stationary storms were allowed to cover the entire planar watershed. Different storm durations were taken such that both equilibrium and partial equilibrium hydrographs were obtained. Both dimensionless flow depth and dimensionless discharge as functions of dimensionless time were computed at different values of dimensionless distance. Figure 5 shows for storm duration equal to 1.8 a typical equlibrium discharge hydrograph at x = 0.25, 0.50, 0.75, and 1.0. For a storm duration of 0.8, Figure 6 shows a typical dimensionless partial equilibrium discharge hydrograph. The hydrograph shape remains the same for different durations in case of equilibrium hydrograph; and

20

the same applies to different durations in case of partial equilibrium hydrograph. For two different durations the dimensionless peak characteristics are exhibited in Table 1. As expected, with storm duration decreasing, the peak flow as well as the time to peak decrease.

6.2 Storms Moving Downstream and Covering the Entire Plane

The storms moving downstream were allowed to cover the entire plane. Two dimensionless storm durations were considered: $T = 1.8$ and 0.8. For each duration two dimensionless storm velocities were used: $V_S = 1.5$ and 3. Thus, four storm cases were considered. For each storm the equilibrium hydrograph for duration equal to 1.8 and partial equilibrium for duration equal to 0.3 were computed. For storm duration equal to 1.8, the discharge hydrograph is shown in Figure 7. For storm duration equal to 0.8, the discharge hydrograph is shown in Figure 8. A summary of results on peak flow an dtime to peak flow is given in Table 1. For the same duration, the storm velocity had virtually no effect on the hydrograph. However, for the same velocity the hydrograph peak decreased with decreasing duartion as the hydrograph changed from an equilibrium situation to a partial equilibrium situation. The effect on the time to peak was less noticeable.

6.3 Comparison of Hydrographs due to Stationary and Downstream-Moving Storms

A comparison of hydrographs corresponding to moving storms of different durations (and velocities) with those of stationary storms of the same duration shows that stationary storms lead to higher or as much peak and longer or as much time to peak. The magnitude of the difference is small but depends on the storm duration. However, even this difference vanishes in case of the equilibrium situation.

6.4 Storms Moving Upstream and Covering the Entire Plane

The storms moving upstream were allowed to cover the entire plane. Two dimensionless storm durations were considered: $T = 1.8$ and 0.8. For each storm duration two dimensionless storm velocities were taken: $V_S = 1.5$ and 3. For each storm the dimensionless depth and discharge were computed. For storm duration equal to 1.8, the discharge hydrograph is shown in Figure 9. For storm duration equal to 0.8, the discharge hydrograph is shown in Figure 10. The peak discharge and time to peak values for four storms are summarized in Table 1. For the same storm duration but different

21

flow velocities the peak discharge remains unaltered but the time to peak decreases with increasing velocity if the hydrograph is the equilibrium hydrograph. In the partial equilibrium situation, the peak discharge increases but the time to peak decreases with increasing velocity.

Table 1. Effect of storm direction and duration on peak flow and time to peak (EH = equilibrium hydrograph; PE = partial equilibrium hydrograph).

Case	Nature of storm	Time to Peak at position x =				Peak discharge at position x =			
Duration/ velocity	Movement	0.25	0.50	0.75	1.0	0.25	0.5	0.75	1.0
1.8, EH	Stationary	0.39	0.63	0.82	1.0	0.25	0.5	0.75	1.0
1.8/1.5, EH	Downstream	0.396	0.63	0.82	1.0	0.25	0.5	0.75	1.0
1.8/10, EH	Downstream	0.396	0.63	0.82	1.0	0.25	0.5	0.75	1.0
1.8/1.5, EH	Upstream	1.06	1.30	1.49	1.67	0.25	0.50	0.75	1.0
1.8/10, EH	Upstream	0.5	0.73	0.93	1.1	0.25	0.5	0.75	1.0
0.8, PE	Stationary	0.396	0.62	0.8	0.8	0.25	0.50	0.75	0.72
0.8/1.5, PE	Downstream	0.396	0.62	0.80	1.02	0.25	0.50	0.71	0.71
0.8/10, PE	Downstream	0.396	0.62	0.80	1.01	0.25	0.50	0.71	0.71
0.8/1.5, PE	Upstream	0.80	0.80	0.80	0.80	0.11	0.195	0.295	0.40
0.8/10, PE	Upstream	0.50	0.73	0.80	0.80	0.25	0.50	0.61	0.64

6.5 Comparison of Hydrographs due to Stationary and Upstream-Moving Storms

A comparison of hydrographs corresponding to upstream-moving storms of different durations with those resulting in stationary storms of the same duration shows that the hydrograph shapes are significantly affected by the storm movement. In general stationary storms lead to lower peaks and shorter time to peak, as shown in Table 1.

6.6 Comparison of Hydrographs due to Downstream-Moving and Upstream-Moving Storms

A comparison of hydrographs shows that the for the same areal coverage and storm duration the peak discharge is lower for storms moving upstream than for storms moving downstream but the reverse is true for the time to peak, if the hydrograph is the partial equilibrium hydrograph. For equilibrium hydrographs the discharge is independent of the storm direction but the time to peak discharge is greater for storms moving upstream than for those moving downstream.

7. APPLICATION FOR STORMS COVERING THE PLANE PARTIALLY

The effect of the direction and duration of storm movement on planar flow was analyzed by considering both moving and stationary storms. The storm velocities were taken as 1, 1.5, 2, 3, 5, and 10 times the normalizing velocity of flow. The planar area covered by a storm was varied as 25, 50, and 75% of the total area. For each velocity, the duration of the storm would be fixed for a fixed areal coverage. In each case, the hydrograph at the downstream end of the plane would be a partial equilibrium one. For purposes of comparison and ease of graphical portrayal it is more convenient to employ dimensionless solutions. To that end the following normalizing quantities were defined as given by equations (63)-(67). The normalizing quantities were in accord with a stationary storm. Using these quantities dimensional solutions were rendered dimensionless. Appendix B contains dimensionless solutions.

7.1 Stationary Storms Covering the Upstream Portion of the Plane

Stationary storms were allowed to cover only a portion (a greater than 0) of the planar watershed. The value of a was taken as a = 0.25, 0.5, and 0.75. For each portion covering a fixed portion, dimensionless flow depth and dimensionless discharge were computed for different covered areas. For purposes of graphical portrayal dimensionless depth and discharge hydrographs were considered at different dimensionless distances measured from the upstream end, including $x = 0.25$, 0.50, 0.75, and 1.0. Figure 13 shows the partial equilibrium discharge hydrograph for a 50% plane

23

coverage and storm duration of 0.333. When the storm duration is increased to 0.5 and the areal coverage to 75%, the discharge hydrograph is shown in Figure 14. As expected, the peak flow increases with increasing covered area and so does the time to peak. Also, the duration of storm plays an important role in determining the hydrograph peak and its time. The peak as well as the time to peak flow decrease with decreasing duartion for the same areal coverage, as shown in Table 2. For the same storm duration, peak flow and time to peak flow increase with increasing areal coverage.

7.2 Storms Moving Downstream

The dimensionless depth and discharge were computed for all storms moving downstream corresponding to to different velocities. Each of these was allowed to cover different portions of the plane (a = 0.25, 0.5, and 0.75). For two sample storms with velocities 1.5 and 3.0, the dimensionless discharge hydrographs. The effect of storm duration and areal coverage on peak flow and its time of occurrence is shown in Table 3. It is seen that as the storm duration increases for the same areal coverage, the peak discharge as well as its time increases. For the same duration when the areal coverage increases, so does the peak discharge but the time to peak decreases.

Table 2. Effect of the duration of stationary storms covering upstream portion of the plane.

Duration/velocity		Storm covering upstream portion							
Areal coverage		Time to peak discharge at x =				Peak discharge at x =			
50%	75%	0.25	0.5	0.75	1.0	0.25	0.5	0.75	1.0
0.167/ 3.0	0.167	0.167	0.57	0.983	0.068	0.068	0.068	0.068	0.068
--	0.25/3.0	0.25	0.25	0.25	0.46	0.125	0.125	0.125	0.125
0.333/ 1.5	--	0.333	0.333	0.622	0.91	0.192	0.192	0.192	0.192
--	0.5/1.5	0.39	0.50	0.50	0.74	0.25	0.35	0.35	0.35

Table 3. Effect of the duration of storms moving downstream and covering the plane partially.

Duration/velocity		Storm moving downstream							
Areal coverage		Time to peak discharge at x =				Peak discharge at x =			
50%	75%	0.25	0.5	0.75	1.0	0.25	0.5	0.75	1.0
0.167/ 3.0	0.167	0.46	0.87	1.28	1.68	0.068	0.068	0.068	0.068
--	0.25/3.0	0.42	0.75	1.05	1.42	0.125	0.125	0.125	0.125
0.333/ 1.5	--	0.40	0.69	0.98	1.27	0.192	0.192	0.192	0.192
--	0.5/1.5	0.39	0.64	0.87	1.11	0.25	0.35	0.35	0.35

7.3 Comparison of Hydrographs due to Stationary and Downstream-Moving Storms

A comparison of hydrographs corresponding to moving storms of different velocities with those of stationary storms covering the same area shows that the hydrograph shape changes significantly for moving storms. This is especially true with the rising part and the peak portion. Also, the timings are changed. As storm velocity rises, the hydrograph tends to appraoch the one due to stationary storms. For the same duration and areal coverage, the peak discharge may remain the same but the time to peak increases for moving storms over that for stationary storms.

Table 4. Effect of the duration of stationary storms covering downstream portion of the plane.

Duration/velocity		Storm covering downstream portion							
Areal coverage		Time to peak discharge at x =				Peak discharge at x =			
50%	75%	0.25	0.5	0.75	1.0	0.25	0.5	0.75	1.0
0.167/ 3.0	0.167	--	--	0.167	0.167	--	--	0.068	0.068
--	0.25/3.0	--	0.25	0.25	0.46	–	0.125	0.125	0.125
0.333/ 1.5	--	--	--	0.333	0 0.333	--	--	0.192	0.192
--	0.5/1.5	--	0.39	0.50	0.50	--	0.35	0.35	0.35

7.4 Stationary Storms Covering the Downstream Portion

Stationary storms were allowed to cover only a portion of the planar area beginning with the downstream side. The value of (1-a) was taken as 0.25, 0.5, and 0.75. For each covered area, dimensionless depth and discharge hydrographs were computed for different covered areas. Figure 17 shows the dimensionless discharge for 50% areal coverage. For 75% areal coverage the discharge hydrograph is graphed in Figure 18. The effect of areal coverage and storm duration is exhibited in Table 4. It is seen that as storm duration increases the peak flow and its time increase for the same areal coverage. For increasing areal coverage but the same storm duration, both the peak flow and time to peak increase.

7.5 Storms Moving Upstream

The dimensionless depth and discharge hydrographs were computed for all storms moving upstream corresponding to different velocities and covered areas. For dimensionless velocity of 1.5, the dimensionless discharge hydrograph is shown in Figures 19. For another dimensionless velocity of 3.0, the discharge hydrographis depicted in Figure20. The effect of the duration of storms moving upstream and covering only a downstream portion is shown in Table 5. As storm duration increases, the peak discharge as well as the time to peak increase for the same areal coverage. For increasing areal coverage but the same duration, both the peak discharge and the time to peak increase.

Table 5. Effect of the duration of storms moving upstream and covering the plane partially.

Duration/velocity		Storm moving upstream							
Areal coverage		Time to peak discharge at x =				Peak discharge at x =			
50%	75%	0.25	0.5	0.75	1.0	0.25	0.5	0.75	1.0
0.167/ 3.0	--	--	--	0.167	0.167	--	--	0.021	0.057
--	0.25/3.0	--	0.25	0.25	0.46	--	0.21	0.057	0.100
0.333/ 1.5	--	--	--	0.333	0.333	--	--	0.049	0.125
--	0.5/1.5	--	0.50	0.50	0.50	--	0.05	0.125	0.215

7.6 Comparison of Hydrographs due to Stationar and Upstream-Moving Storms

A comparison of discharge hydrographs for moving storms with those due to stationary storms shows that the hydrograph shapes are significantly affected by the storm movement. The peak discharge is higher for stationary storms than it is for storms moving upstream but the time to peak remains unaltered for the same duration as well as for the same coverage.

7.7 Comparison of Hydrographs due to Downstream-Moving and Upstream-Moving Storms

A comparison of hydrographs due to storms moving downstream with those due to storms moving upstream shows that the hydrograph shape is significantly influenced by the direction of storm movement. This is especially the case with the time of delivery of water at the basin outlet. Looking at Tables 3 and 5, it is concluded that for the same areal coverage and storm duration the hydrograph peak is higher for downstream moving storms than it is for upstream moving storms. The same is true for the time to peak flow.

8. CONCLUSIONS

The following conclusions can be drawn from this study: (1) The hydrograph shape is significantly affected by the direction of the storm movement. (2) The timing of the discharge delivery at the outlet is influenced by the direction of storm movement. (3) For the same duration of storm, the peak discharge is greater for storms moving downstream than that for storms moving upstream. (4) For same storm duration, the time to peak occurs much later for storms moving upstream than for storms moving downstream. (5) Stationary storms, in general, produce higher peak discharge and lower time to peak than moving storms. (6) For the same areal coverage and the same duration of storm, the peak discharge is greater for storms moving downstream than that for storms moving upstream. (7) For same areal coverage and storm duration, the time to peak occurs much later for storms moving upstream than for storms moving downstream.

APPENDIX A: DIMENSIONLESS SOLUTION FOR MOVING STORMS FULLY COVERING THE PLANE

When dimensionless quantities are substituted in equation (5), the governing equation in dimensionless form takes the form:

$$\frac{\partial h^*}{\partial t^*} + n h^{*n-1} \frac{\partial h^*}{\partial x^*} = 1 \qquad \text{(A.1)}$$

27

Its characteristic equations are

$$\frac{dh^*}{dx^*} = \frac{1}{nh^{*n-1}} \tag{A.2}$$

$$\frac{dt^*}{dx^*} = \frac{1}{nh^{*n-1}} \tag{A.3}$$

For simplicity superscript (*) is dropped henceforth but the quantities remain dimensionless unless otherwise stated.

A.1   Planar Flow due to Storms Moving Downstream: Equilibrium Hydrograph

$$h(x_0, \frac{x_0}{V_s}) = 0 \quad , \quad 0 \le x_0 \le 1 \tag{A.4}$$

A.1.1 Domain D_1 **:** The initial condition is

$$h(x, x_0) = (x - x_0)^{1/n} \tag{A.5}$$

$$t(x, x_0) = \frac{x_0}{V_s} + (x - x_0)^{1/n} \tag{A.6}$$

The solution of equations (A.2) and (A.3), subject to equation (A.4), is

Eliminating x_0 between equations (A.5) and (A.6), the flow depth, as a function of x and t, can be expressed as

28

$$h^n = h V_s + x - t V_s \qquad \text{(A.7)}$$

and flow discharge as

$$Q(x,t) = h^n \qquad \text{(A.8)}$$

A.1.2 Domain D_2: The boundary condition is

$$h(0,t_0) = h_0 = 0 \qquad \text{(A.9)}$$

The solution of equations (A.2) and (A.3), subject to equation (A.9), is

$$h(x,t_0) = x^{1/n} \qquad \text{(A.10)}$$

$$t(x,t_0) = t_0 + x^{1/n} \qquad \text{(A.11)}$$

The flow depth, as a function of x and t, can be expressed as

$$h(x,t) = x^{1/n} \qquad \text{(A.12)}$$

$$Q(x,t) = x \qquad \text{(A.13)}$$

and discharge as

A.1.3 Domain D_3: The initial condition is given by equation (A.10) with x replaced by x_0^*, $0 \le x_0^* \le 1$:

$$h(x_0^*) \;=\; h_0 \;=\; x_0^{*\,1/n} \tag{A.14}$$

The solution of equations (A.2) and (A.3), subject to equation (A.14), is

$$h(x,x_0^*) = h_0 = x_0^{*\,1/n} \tag{A.15}$$

$$t(x,x_0) = T + \frac{1}{n}\,(x_0^*)^{-(n-1)/n}(x - x_0) \tag{A.16}$$

The flow depth, as a function of x and t, can be written as

$$t = T + \frac{1}{n}\,h^{-(n-1)}(x - h^{\,n}) \tag{A.17}$$

and discharge as

$$Q(x,t) = h^{\,n} \tag{A.18}$$

A.2 Planar Flow due to Storm Movement Downstream: Partial Equilibrium Hydrograph

A.2.1 <u>Domain D_1</u>: The solution is given by equations (A.5) and (A.6).

A.2.2 <u>Domain D_2</u>: The solution is given by equations (A.10) and (A.11).

A.2.3 <u>Domain D_{3A}</u>: The solution is given by equations (A.15) and (A.16). Here $0 \le x_0^* \le \bar{x}$.

A.2.4 <u>Domain D_{3B}</u>: The initial condition is given by equation (A.5) with x replaced by x_0^*, $\bar{x} \le x_0^* \le 1$:

$$h(x,x_0^*) = (x_0^* - x_0)^{1/n} \tag{A.19}$$

The solution of equations (A.2) and (A.3), subject to equation (A.19), follows:

$$h(x,x_0^*) = h_0 = (x_0^* - x_0)^{1/n} \tag{A.20}$$

$$t(x,x_0^*) = \frac{1}{V_s} + \frac{1}{n}(x_0^* - x_0)^{-(n-1)/n}(x - x_0^*) \tag{A.21}$$

$$\frac{1}{V_s} = \frac{x_0}{V_s} + (x_0^* - x_0)^{1/n} \tag{A.22}$$

The link between x_0 and x_0^* is given by equation (A.6) with x replaced by x_0^* and t by $1/V_S$:

The flow depth, as a function of x and t, can be expressed as

This is an inverted expression of h as a function of x and t.

$$t = \frac{1}{V_s} + \frac{1}{n}h^{-(n-1)}(x - h^n - 1 + hV_s) \tag{A.23}$$

A.3 Planar Flow due to Storms Moving Upstream: Equilibrium Hydrograph HYDROGRAPH

A.3.1 Domain D$_1$: The initial condition is given by

$$h(x_0, \frac{1-x_0}{V_S}) = 0 \tag{A.24}$$

In this domain, $0 \le x_0 \le 1$, where x_0 is the point of origination on $t = (1-x)/V_S$ of the characteristic intersecting the line $t=(1-x)/V_S$. The solution of equations (A.2) and (A.3), subject to equation (A.24), is given as

31

$$h(x, x_0) = (x - x_0)^{\frac{1}{n}} \tag{A.25}$$

$$t(x, x_0) = \frac{1 - x_0}{V_S} + (x - x_0)^{\frac{1}{n}} \tag{A.26}$$

Eliminating x_0 between equations (A.25) and (A.26), the flow depth, as a function of x and t, can be expressed as

$$h^n + V_S h = x + t V_S - 1 \tag{A.27}$$

A.3.2 Domain D_{1B}: In this case $(1/V_S) \le t_0 \le T$. The initial condition is given by:

$$h(0, t_0) = 0 \tag{A.28}$$

The solution of equations (A.2) and (A.3), subject to equations (A.28), follows:

$$h(x, t_0) = x^{\frac{1}{n}} \tag{A.29}$$

$$t(x, t_0) = t_0 + x^{\frac{1}{n}} \tag{A.30}$$

One can write

$$h(x, t) = x^{\frac{1}{n}} \tag{A.31}$$

$$Q(x, t) = x \tag{A.32}$$

A.3.3 Domain D_3 :The initial condition is given by equation (A.29) with x replaced by x_0^* and t_0

replaced by T:

$$h(x_0, T) = x_0^{*\frac{1}{n}}$$ (A.33)

The solution of equations (A.2) and (A.3), subject to equation (A.33), is

$$h(x, x_0^*) = x_0^{*\frac{1}{n}}$$ (A.34)

$$t(x, x_0^*) = T + x_0^{*-(n-1)/n} (x - x_0^*)$$ (A.35)

A.4 Planar Flow for Storms Moving Upstream: Partial Equilibrium Hydrograph

A.4.1 Domain D$_1$: The solution is given by equations (A.25) and (A.26).

A.4.2 Domain D$_2$: The solution is given by equations (A.29) and (A.30).

A.4.3 Domain D$_{3A}$: The solution is given by equations (A.34) and (A.35). Here $0 \leq x_0^* \leq \bar{x}$.

A.4.4 Domain D$_{3B}$: Here $\bar{x} \leq x_0^* \leq 1$. The initial condition is given by equation (A.25) with x replaced by x_0^*:

$$h(x_0, x_0^*) = (x_0^* - x_0)^{\frac{1}{n}}$$ (A.36)

The solution of equations (A.2) and (A.3), subject to equations (A.36), is given as

$$h(x, x_0^*) = h(x_0, x_0^*) = (x_0^* - x_0)^{\frac{1}{n}}$$ (A.37)

The connection between x_0 and x_0^* is given by equation (A.26) as

$$t(x,x_0^*) = T + \frac{1}{n}(x-x_0^*)(x_0^* - x_0)^{-\frac{(n-1)}{n}} \quad\quad (A.38)$$

$$t(x_0^*) = T + \frac{1-x_0}{V_S} + (x_0^* - x_0)^{\frac{1}{n}} \quad\quad (A.39)$$

APPENDIX B: DIMENSIONLESS SOLUTIONS FOR MOVING STORMS PARTIALLY COVERING THE PLANE

When dimensionless quantities are substituted in equation (5), the governing equation in dimensionless form becomes equation (A.1) whose characteristic equations are given by equations (A.2) and (A.3). For simplicity superscript (*) is dropped henceforth but the quantities remain dimensionless unless otherwise stated.

B.1 Planar Flow due to Storm Movement Downstream

B.1.1 <u>Domain</u> D_1: The initial condition is given by equation (A.4) with $0 \le x_0 \le a$. The solution is given by equations (A.5) and (A.6), or equations (A.7) and (A.8).

B.1.2 <u>Domain</u> D_2: The boundary condition is given by equation (A.9) and the solution by equations (A.10) and (A.11), or equations (A.12) and (A.13).

B.1.3 <u>Domain D_{3A}</u>: The initial condition is given by equation (A.10) with x replaced by x_0^*, $0 \le x_0^* \le \bar{x}$, which becomes equation (A.14). The solution for this domain is given by equations (A.15) and

$$t(x,x_0) = \frac{a}{V_S} + \frac{1}{n}(x_0^*)^{-(n-1)/n}(x-x_0) \quad\quad (B.1)$$

The flow depth, as a function of x and t, can be written as

and discharge by equation (A.18).

B.1.3 **Domain D_{3B}:** The initial condition is given by equation (A.5) with x replaced by x_0^*, $\bar{x} \le x_0^* \le aL$, which becomes equation (A.19). The solution of equations (A.2) and (A.3),

$$t = \frac{a}{V_S} + \frac{1}{n} h^{-(n-1)} (x - h^n) \tag{B.2}$$

subject to equation (A.19), follows:

$$h(x, x_0^*) = h_0 = (x_0^* - x_0)^{1/n} \tag{B.3}$$

$$t(x, x_0^*) = \frac{a}{V_s} + \frac{1}{n} (x_0^* - x_0)^{-(n-1)/n} (x - x_0^*) \tag{B.4}$$

$$\frac{a}{V_s} = \frac{x_0}{V_s} + (x_0^* - x_0)^{1/n} \tag{B.5}$$

The link x_0 and x_0^* is given by equations (A.6) with x replaced by x_0^* and t by a/ V_S:

The flow depth, as a function of x and t, can be expressed as

$$t = \frac{a}{V_s} + \frac{1}{n} h^{-(n-1)} (x - h^n - 1 + h V_s) \tag{B.6}$$

This is an inverted expression of h as a function of x and t.

B.1.3 **Domain D_{4B}:** The boundary condition is given by equations (A.42) and (A.43):

$$h(a, x_0^*) = h_0 = (x_0^* - x_0)^{1/n} \tag{B.7}$$

35

$$\overline{s_0} = \frac{a}{V_s} + \frac{1}{n}(\overline{x})^{-(n-1)/n}(a - x_0^*)$$ (B.9)

$$s_0 = \frac{a}{V_s} + \frac{1}{n}(x_0^* - x_0)^{-(n-1)/n}(a - x_0^*)$$ (B.8)

The solution in this domain is given by equation (A.42) and

$$t(x, s_0) = s_0 + \frac{1}{n}(x_0^* - x_0)^{-(n-1)/n}(x - a)$$ (B.10)

B.1.3 Domain D_{4A}: The boundary condition is given by

$$h(a, x_0^*) = h_0 = (x_0^*)^{1/n}$$ (B.11)

$$s_0 = \frac{a}{V_s} + \frac{1}{n}(x_0^*)^{-(n-1)/n}(a - x_0^*)$$ (B.12)

where $\overline{s_0}$ is given by equation (B.8) and $s_0 \geq \overline{s_0}$. The solution in this domain is given by equation

(B.1) and

$$t(x, s_0) = s_0 + \frac{1}{n}(x_0^*)^{-(n-1)/n}(x - a)$$ (B.13)

B.2 Planar Flow for Storms Moving Upstream

B.1.1 Domain D_1: The initial condition is given by equation (A.24) with $1 \leq x_0 \leq x$, where x is the

point of origination on $t = (1-x)/V_S$. The solution is given by equations (A.25) and (A.26). The flow

depth as a function of x and t is given by equation (A.27). The value of $\bar{x}$ is determined from equation (A.26) when x_0 is replaced by $\bar{x}$, x by 1, and t by $(1-a)/V_s$:

$$\bar{x} - (1 - \bar{x})^{1/n} = a \qquad \text{(B.14)}$$

B.1.2 Domain D_{1B}**:** In this case, $a \leq x_0 \leq \bar{x}$. The solution is given by equations (A.25) and (A.26).

B.1.3 Domain D$_3$: The parameter is x_0^* , $a \leq x_0^* \leq \bar{x}$. The initial condition is given the solution in domain D$_{1A}$ [by equation (A.42)] with x replaced by x_0^* in equation (A.36). The solution for this domain is given by equations (A.37) and

$$t(x, x_0) = \frac{1 - a}{V_s} + \frac{1}{n}(x_0^* - x_0)^{-(n-1)/n}(x - x_0^*) \qquad \text{(B.15)}$$

The connection between x_0 and x_0^* is given by equation (A.26):

$$t(x_0^*) = \frac{1 - x_0}{V_s} + (x_0^* - x_0)^{1/n} \qquad \text{(B.16)}$$

ACKNOWLEDGMENT

REFERENCES

Foroud, N., Broughton, R.S. and Austin, G.L., 1984. The effects of a moving rainstorm on direct runoff properties. Water Resources Bulletin, Vol. 20, No. 1, pp. 87-91.

Jensen, M., 1984. Runoff pattern and peak flows from moving block rains based on a linear time-area curve. Nordic Hydrology, Vol. 15, pp. 155-168.

Marcus, N., 1968. A laboratory and analytical study of surface runoff under moving rainstorms. Unpublished Ph.D. thesis, University of Illinois, Urbana, Illinois.

Maksimov, V.A., 1964. Computing runoff produced by a heavy rainstorm with a moving center. Soviet Hydrology, No. 5, pp. 510-513.

Niemczynowicz, J., 1984a. Investigation of the influence of rainfall movement on runoff hydrograph: Part I. Simulation of conceptual cathcment. Nordic Hydrology, Vol. 15, pp. 57-70.

Ngirane-Katashaya, G.G. and Wheater, H.S., 1985. Hydrograph sensitivity to storm kinematics. Water Resources Research, Vol. 21, No. 3, pp. 337-345.

Niemczynowicz, J., 1984b. Investigation of the influence of rainfall movement on runoff hydrograph: Part II. Simulation of real catchments in the city of Lund. Nordic Hydrology, Vol. 15, pp. 71-84.

Ogden, F.L., Richardson, J.R. and Julien, P.Y., 1995. Similarity in catchment response: 2. Moving rainstorms. Water Resources Research, Vol. 31, No. 6, pp. 1543-1547.

Roberts, M.C. and Klingeman, P.C., 1970. The influence of landform and precipitation   parameters on flood hydrographs. Journal of Hydrology, Vol. 11, pp. 393-411.

Sargent, D.M., 1981. An investigation into the effects of storm movement on the design of urban drainage systems: Part 1. The Public Health Engineer, Vol. 9, pp. 201-207.

Sargent, D.M., 1982. An investigation into the effects of storm movement on the design   of urban drainage systems: Part 2. Probability analysis. The Public Health Engineer, Vol. 10, No. 2, pp. 111-117.

Singh, V.P. 1996. Kinematic Wave Modeling in Water Resources: Surface Water Hydrology. John Wiley, New York, 1399 pp.

Singh, V.P.,1997a. Effect of spatial and temporal variability in rainfall and watershed characteristics on streamflow hydrograph. Hydrological Processes, Vol. 11, pp. 1649-1669.

Singh, V.P., 1998. Effect of the direction of storm movement on planar flow. Hydrological Processes, Vol. 12, pp. 147-170.

Stephenson, D., 1984. Kinematic study of effects of storm dynamics on runoff hydrographs. Water SA, Vol. 10, No. 4, pp. 189-196.

Surkan, A.J., 1974. Simulation of storm velocity effects of flow from distributed channel network. Water Resources Research, Vol. 10, No. 6, pp. 1149-1160.

Yen, B.C. and Chow, V.T., 1968. A study of surface runoff due to moving rainstorms. Hydraulic Engineering Series No. 17, 112 p., Department of Civil Engineering, University of Illinois, Urbana, Illinois.

Figure Captions:
Figure 1. Solution domain for a storm moving downstream: equilibrium hydrograph.
Figure 2. Solution domain for a storm moving downstream: partial equlibrium hydrograph.
Figure 3. Solution domain for a storm moving upstream: equilibrium hydrograph.
Figure 4. Solution domain for a storm moving upstream: partial equilibrium hydrograph.
Figure 5. Dimensionless discharge hydrographs at different locations due to a stationary storm occurring for a dimensionless duration of 1.8.
Figure 6. Dimensionless discharge hydrographs at different locations due to stationary storm occurring for a dimensionless duration of 0.8.
Figure 7. Dimensionless equilibrium discharge hydrographs at different locations due to a storm moving downstream and occurring for a dimensionless duration of 1.8.
Figure 8. Dimensionless partial equilibrium discharge hydrographs at different locations due to a storm moving downstream and occurring for a dimensionless duration of 0.8.
Figure 9. Dimensionless equilibrium discharge hydrographs at different locations due to a storm moving upstream and occurring for a dimensionless duration of 1.8.
Figure 10. Dimensionless partial equilibrium discharge hydrographs at different locations due to a storm moving upstream and occurring for a dimensionless duration of 0.8.
Figure 11. Solution domain for a storm moving downstream.
Figure 12. Solution domain for a storm moving upstream.
Figure 13. Dimensionless discharge hydrographs at different locations due to a stationary storm Covering 50% of the plane and occurring for a dimensionless duration of 0.333.
Figure 14. Dimensionless discharge hydrographs at different locations due to a stationary storm Covering 75% of the plane and occurring for a dimensionless duration of 0.5.
Figure 15. Dimensionless discharge hydrographs at different locations due to a storm moving downstream covering 50% of the plane and occurring for a dimensionless duration of 0.333.
Figure 16. Dimensionless discharge hydrographs at different locations due to a storm moving downstream covering 75% of the plane and occurring for a dimensionless duration of 0.5.
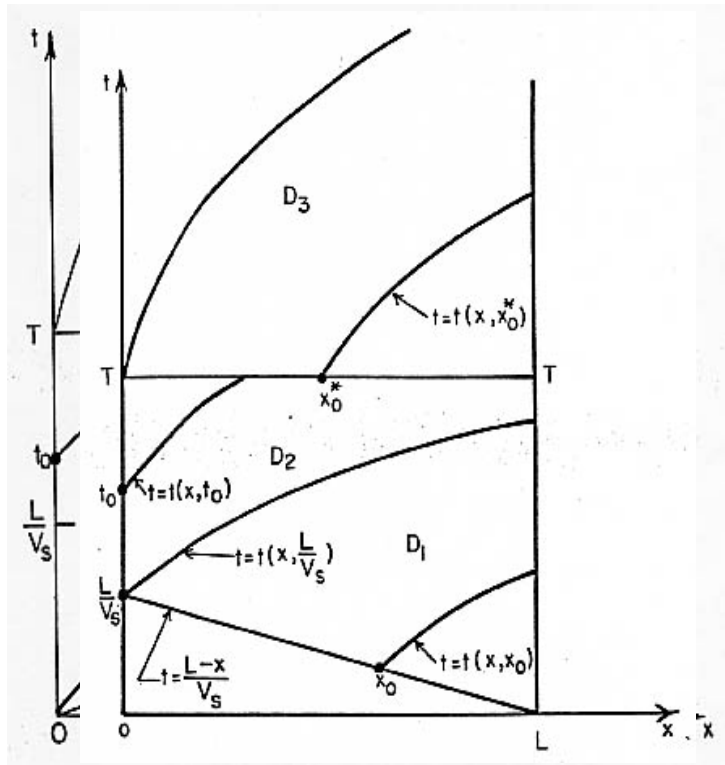**Figure 17.** Dimensionless discharge hydrographs at different locations due to a stationary storm Covering 50% of the plane on the down stream side and occurring for a dimensionless duration of 0.333.
Figure 18. Dimensionless discharge hydrographs at different locations due to a stationary storm Covering 75% of the plane on the down stream side and occurring for a dimensionless duration of 0.333.
Figure 19. Dimensionless discharge hydrographs at different locations due to a storm moving upstream covering 50% of the plane and occurring for a dimensionless duration of 0.333.
Figure 20. Dimensionless discharge hydrographs at different locations due to a storm moving upstream covering 75% of the plane and occurring for a dimensionless duration of 0.5.

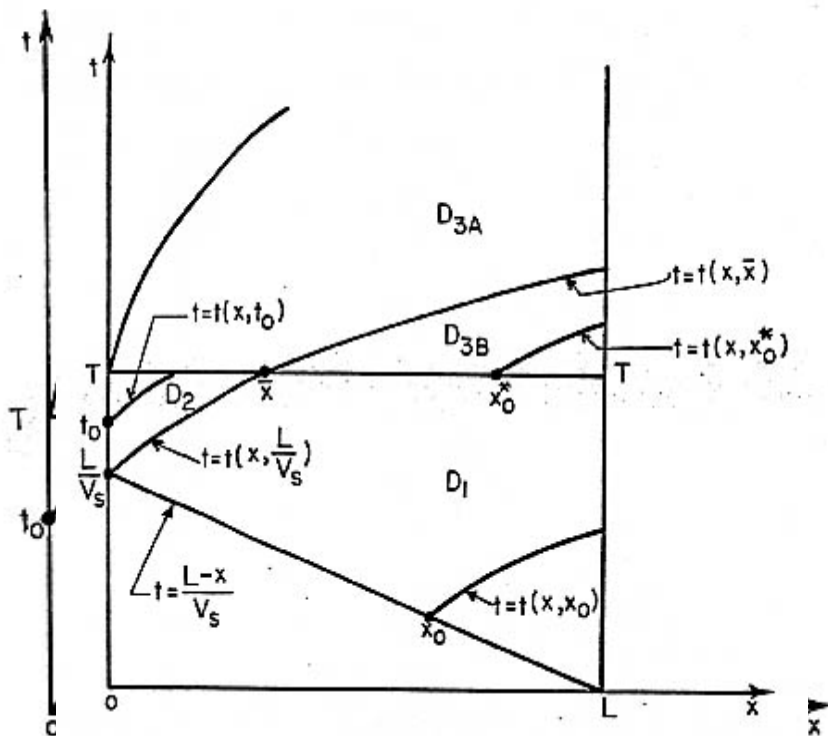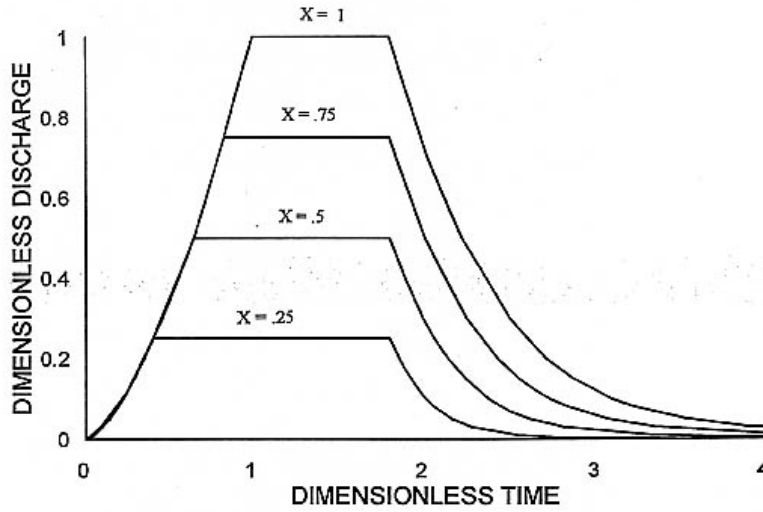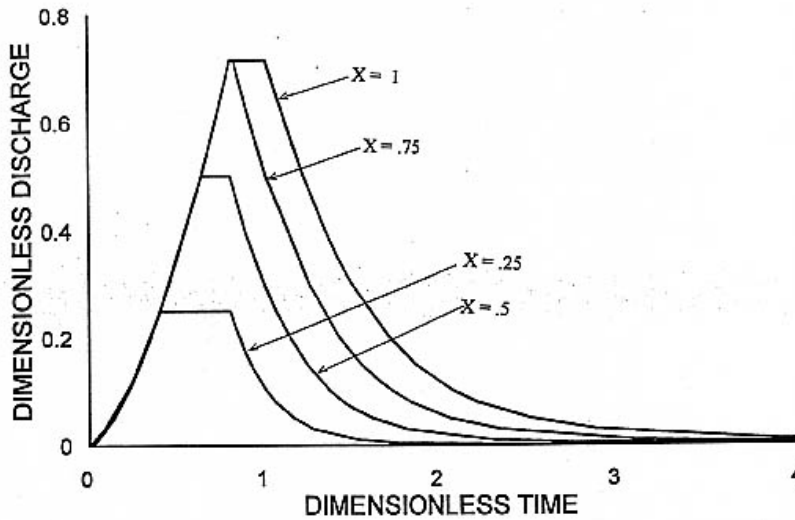**Figure 3** Solution domain for a storm moving
downstream: partial equilibrium hydrograph.

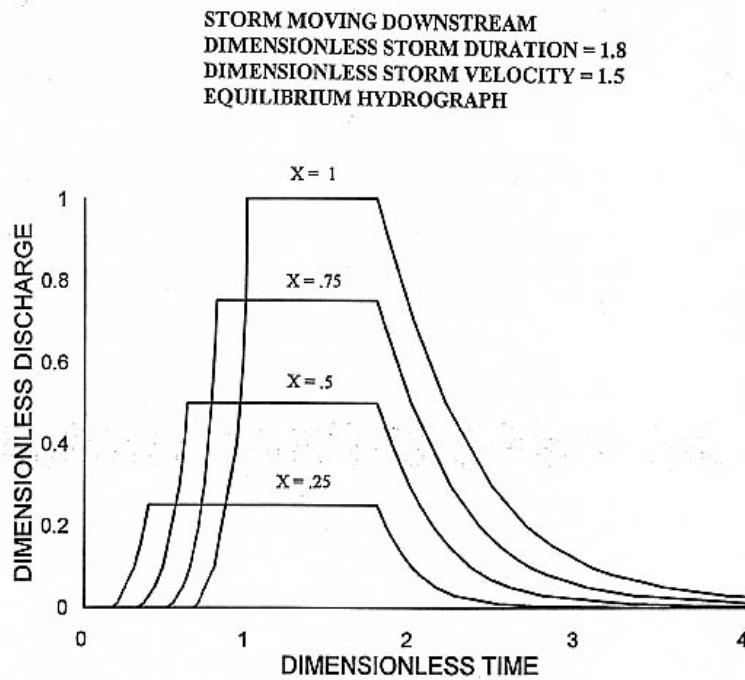**Figure 2** Solution domain for a storm moving downstream:
equilibrium hydrograph.

Figure 5 Dimensionless discharge hydrographs at different locations due to a stationary storm occurring for a dimensionless duration of 1.8.
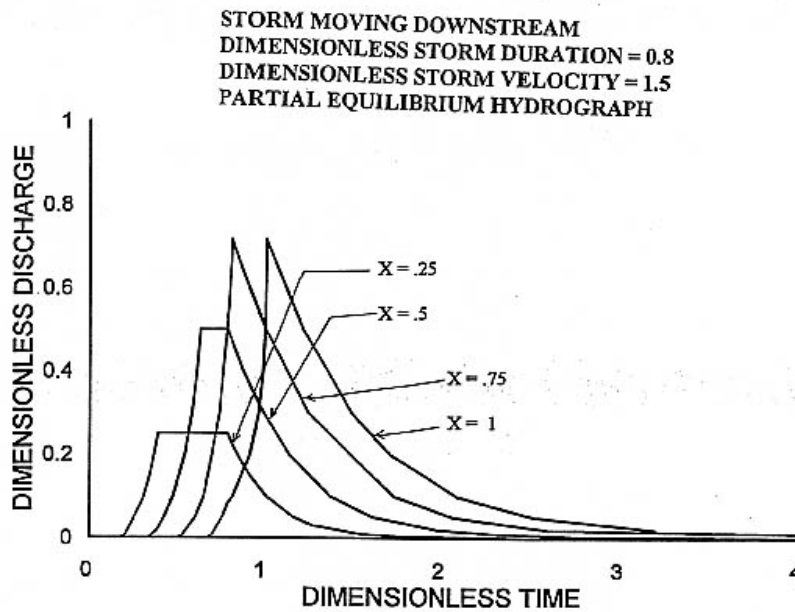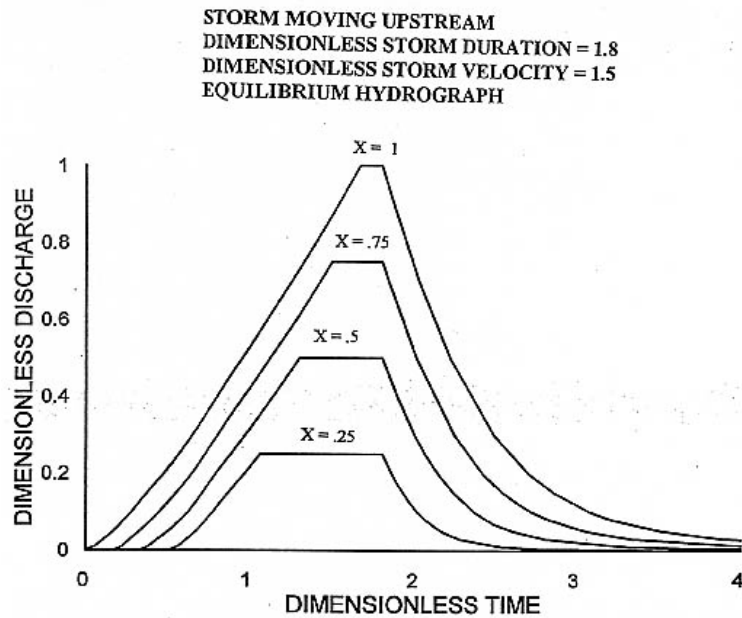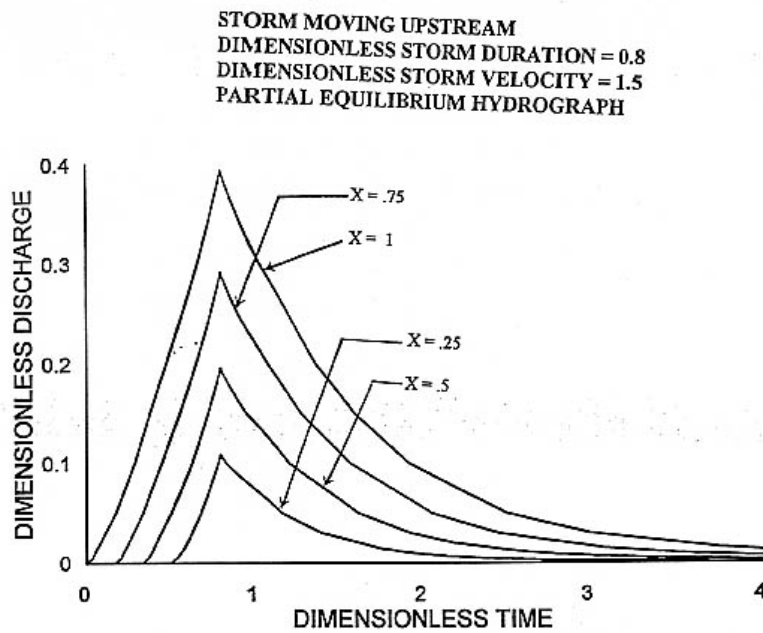

Figure 6 Dimensionless discharge hydrographs at different locations due to stationary storm occurring for a dimensionless duration of 0.8.

Figure 7 Dimensionless equilibrium discharge hydrographs at different locations due to a storm moving downstream and occurring for a dimensionless duration of 1.8.

Figure 8 Dimensionless partial equilibrium discharge hydrographs at different locations due to a storm moving downstream and occurring for a dimensionless duration of 0.8.
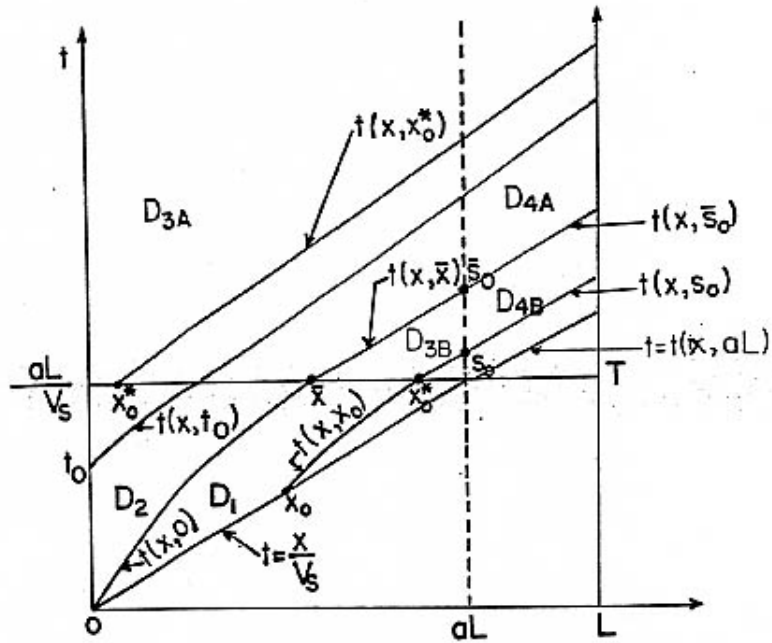
STORM MOVING UPSTREAM
DIMENSIONLESS STORM DURATION = 1.8
DIMENSIONLESS STORM VELOCITY = 1.5
EQUILIBRIUM HYDROGRAPH

Figure 9 Dimensionless equilibrium discharge hydrographs at different locations due to a storm moving upstream and occurring for a dimensionless duration of 1.8.

STORM MOVING UPSTREAM
DIMENSIONLESS STORM DURATION = 0.8
DIMENSIONLESS STORM VELOCITY = 1.5
PARTIAL EQUILIBRIUM HYDROGRAPH

Figure 10 Dimensionless partial equilibrium discharge hydrographs at different locations due to a storm moving upstream and occurring for a dimensionless duration of 0.8

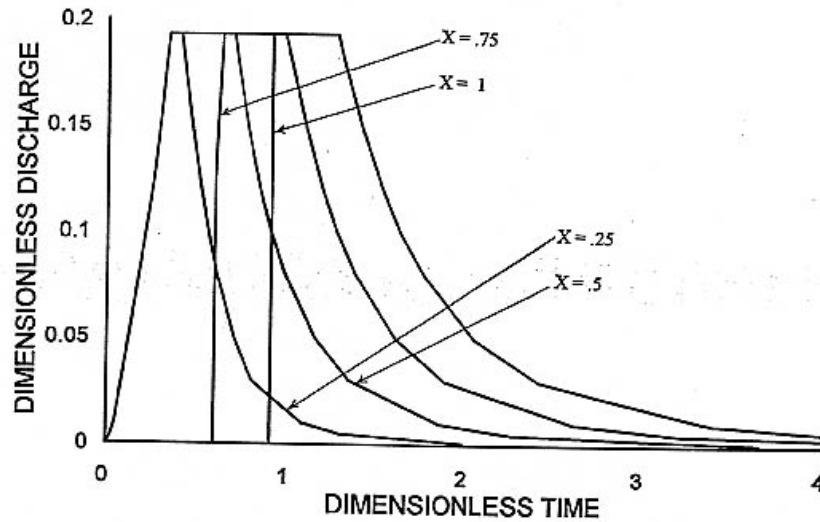**Figure 11** Solution domain for a storm moving
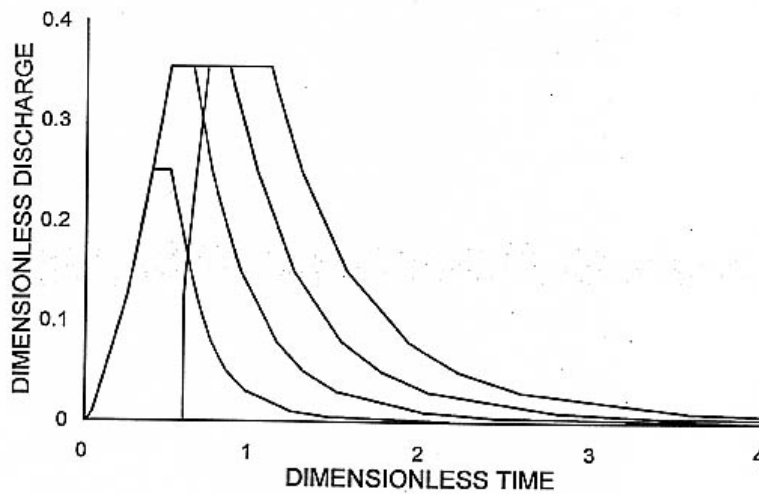downstream.

Figure 12 Solution domain for a storm moving upstream.

44

STATIONARY STORM COVERING 50% OF THE UPSTREAM PLANE
DIMENSIONLESS STORM DURATION = 0.333

Figure 13 Dimensionless discharge hydrographs at different locations due to a stationary storm. Covering 50% of the plane and occurring for a dimensionless duration of 0.333.
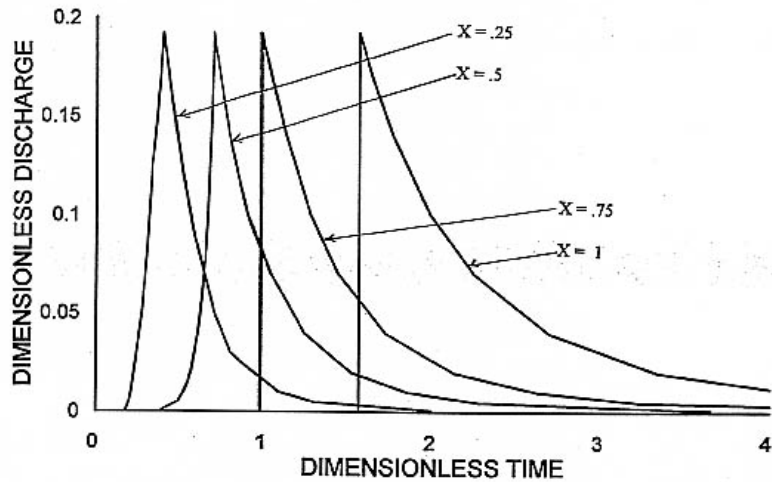

STATIONARY STORM COVERING 75% OF THE UPSTREAM PLANE
DIMENSIONLESS STORM DURATION = 0.50

Figure 14 Dimensionless discharge hydrographs at different locations due to a stationary storm. Covering 75% of the plane and occurring for a dimensionless duration of 0.5.
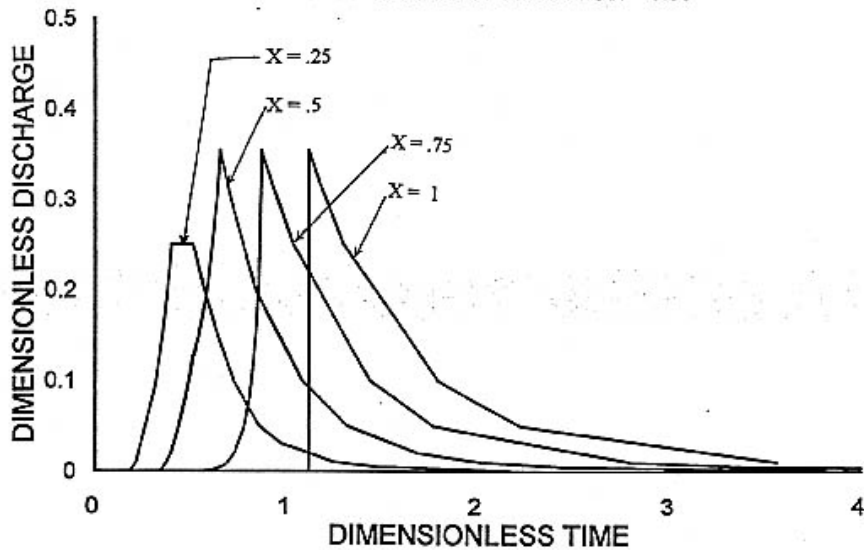
45

Figure 15 Dimensionless discharge hydrographs at different locations due to a storm moving downstream covering 50% of the plane and occurring for a dimensionless duration of 0.333.
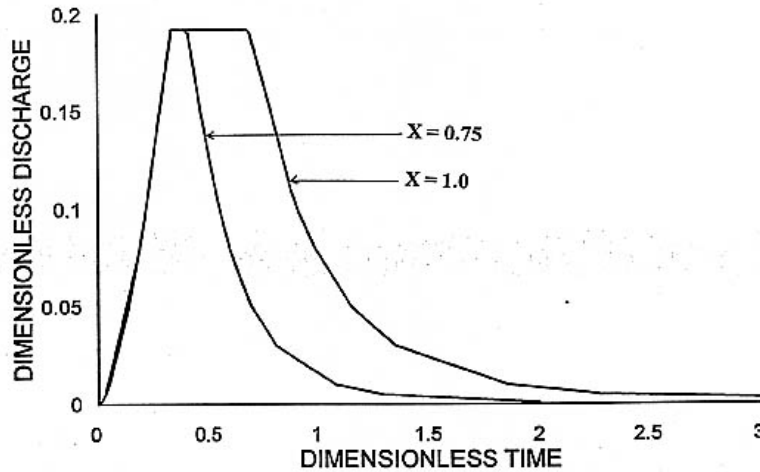

Figure 16 Dimensionless discharge hydrographs at different locations due to a storm moving downstream covering 75% of the plane and occurring for a dimensionless duration of 0.5.

46

STATIONARY STORM COVERING 50% OF THE DOWNSTREAM PART
OF THE PLANE
DIMENSIONLESS STORM DURATION = 0.33

Figure 17 Dimensionless discharge hydrographs at
different locations due to a stationary storm. Covering 50%
of the plane on the down stream side and occurring for a
dimensionless duration of 0.333.

STATIONARY STORM COVERING 75% OF THE DOWNSTREAM PART
OF THE PLANE
DIMENSIONLESS STORM DURATION = 0.50

Figure 18 Dimensionless discharge hydrographs at different
locations due to a stationary storm. Covering 75% of the plane on
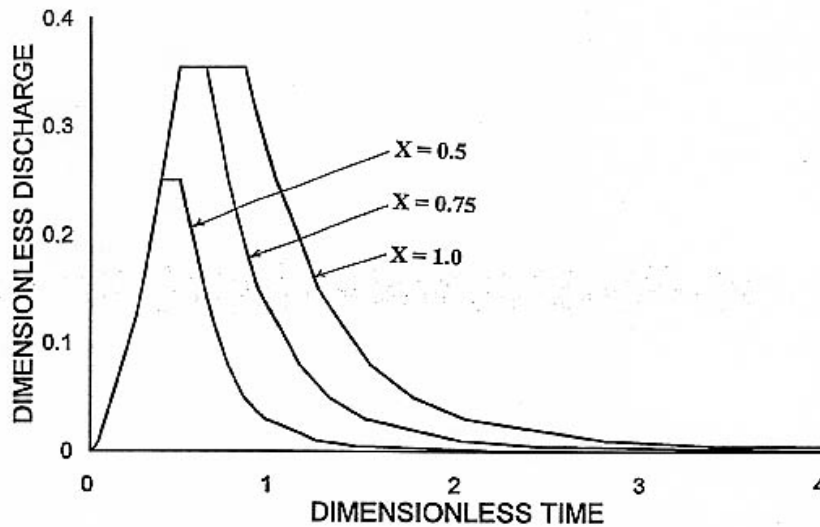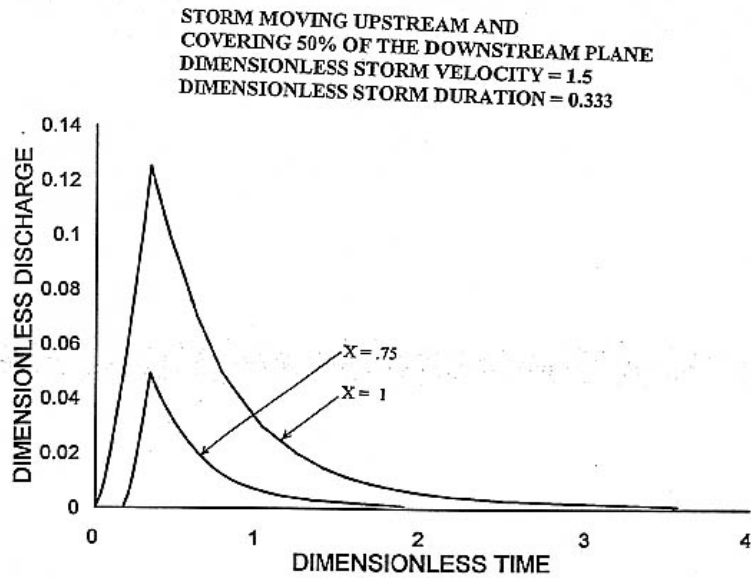the down stream side and occurring for a dimensionless
duration of 0.333.

47

Figure 19 Dimensionless discharge hydrographs at different locations due to a storm moving upstream covering 50% of the plane and occurring for a dimensionless duration of 0.333.
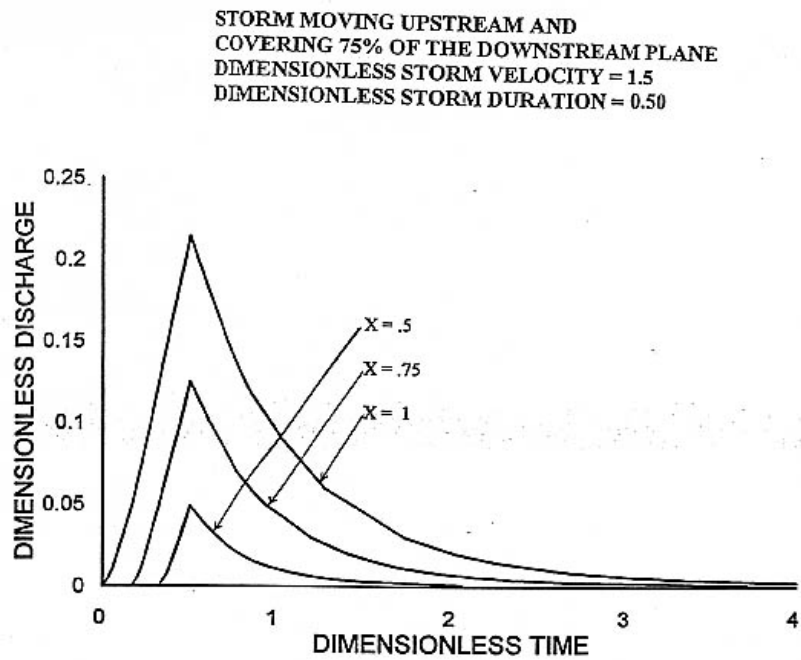
Figure 20 Dimensionless discharge hydrographs at different locations due to a storm moving upstream covering 75% of the plane and occurring for a dimensionless duration of 0.5.

Basic Information

Title:	Denitrification in Wetlands Receiving Mississippi River Freshwater Diversion: Water Quality Aspects
Project Number:	GR02673 C-03 FY00
Start Date:	3/1/2000
End Date:	2/28/2001
Research Category:	Water Quality
Focus Category:	Water Quality, Non Point Pollution, Nitrate Contamination
Descriptors:	Water quality, freshwater diversion, nitrogen, biogeochemistry
Lead Institute:	Louisiana Water Resources Research Institute
Principal Investigators:	Ronald D. DeLaune, Charles W. Lindau

Publication

Denitrification in Water Bodies Receiving Mississippi River Freshwater Diversion

Final Report To Louisiana Water Resources Research Institute

R.D. DeLaune, C.W. Lindau, A. Jugsujinda and R.R. Iwai
Louisiana State University Wetland Biogeochemical Institute
Baton Rouge, Louisiana
70803-7511

Abstract

Nitrate levels in Mississippi River waters has tripled in the past several decades. Excessive nutrients in the Mississippi River are contributing water quality issues along the Louisiana Gulf Coast. In addition, as a result of restoration efforts to counteract the extensive wetland loss in coastal Louisiana the state of Louisiana has developed a plan of freshwater diversion that will mimic flood events of the Mississippi River. There has been controversy about the effects of such diversion into Louisiana coastal wetlands because of possible eutrophication as is currently observed in offshore waters. In this study denitrification or rate of nitrate removed was determined in sediment-water columns of Big Mar, a open water body currently receiving diverted Mississippi water from the Caernarvon diversion structure which introduces freshwater into Brenton Sound Estuary and in sediment-water columns of Lake Cataouatcha, the receiving water body at the Davis Pond Diversion which in the near future will introduce freshwater into the Barataria Basin.

Measured nitrate removal in sediment-water columns showed the two sites had a large potential for denitrification and nitrogen removal (assimilation and immobilization). Measured rates suggest that most of the nitrate in diverted Mississippi River water would be removed in the upper reaches of Barataria Basin and Brenton Sound Estuary.

Introduction

As a result of restoration efforts to counteract the extensive wetland loss in coastal Louisiana the state of Louisiana has developed a plan of freshwater diversion that will mimic flood events of the Mississippi River. There has been controversy about the effects of such diversion into Louisiana coastal wetlands because of possible eutrophication as is currently observed in offshore waters. Such Mississippi River freshwater diversion projects (six diversions currently in operation) also introduce agricultural chemicals found in Mississippi River waters. By siphoning, pumping or cutting through lower levees, diversion projects are moving millions of gallons of water from the Mississippi River into wetlands and estuaries. The infusion of freshwater and sediment will offset submergence, bring essential nutrients and reduce salinity levels in wetlands allowing for enhanced vegetation growth. The Caernarvon structure constructed in 1991 located on the east bank of the Mississippi River below New Orleans currently introduces up to 8,000 cubic feet per sec (cfs) of freshwater into adjacent wetlands in Breton Sound Estuary.

The introduction of Mississippi River water into Louisiana coastal wetlands can introduce nutrients which can impact water quality of estuaries. Nitrogen is currently applied to agricultural lands in the Mississippi Drainage Basin at a rate of four times that which was applied in 1940. The amount of nitrate in the Mississippi River has triple during that period (Turner and Rabalais, 1994). Approximately 45 percent of the nitrate that reaches the lower Mississippi River appear to be entering from the upper portion of the river. Only 7 percent of the nitrate is from the Lower Mississippi River (Antweiler et al., 1995). The U.S. Geological Survey reports that once the nitrate enters the river, it apparently remains in the river valley. Nitrate-N in the Mississippi

River at New Orleans is on the order of 100 µg/l. Between April 1991 and April 1992, the Mississippi River delivered 900,000 metric tons of nitrates to the Gulf of Mexico (Antweiler et al., 1995).

Since 1991, Mississippi River water has been diverted at Caernarvon, Louisiana, into Breton Sound Estuary. Loading rates of nitrite + nitrate N (5.6 – 13.4 g N m^{-2} yr^{-1}) and total nitrogen (8.9 – 23.4 g N m^{-2} yr^{-1}) entering the northern portion of the estuary have been reported by Lane et al. (1999).

In this study, we quantify denitrification of nitrate at two wetland sites, Big Mar, currently receive nitrogen input as result of Mississippi River water (Caernarvon freshwater diversion) and a site (Davis Pond) which is scheduled to receive diverted Mississippi River water. Denitrification rate in sediment was quantified using acetylene blockage technique, we determined reduction in NO_3^- concentration in overlying water and present data on N_2O fluxes from open-water wetlands, as affected by excessive NO_3^- in waters.

Materials and Methods

Site A - Caernarvon Diversion (Big Mar)

Caernarvon, about 100 miles south of Baton Rouge, Louisiana (Latitude 29.8227 N, Longitude 89.92175 W), was selected as one location for this study. Cores were collected from Big Mar, an abandoned agricultural site. Due to failure of levee and pumping system the area reverted to open water. Freshwater from the Mississippi is currently diverted directly into Big Mar, which drains through a series of channels into marsh in upper Breton Sound Estuary.

Laboratory Procedures

Fresh sediments collected from the top 30 cm of the Big Mar Lake were mixed homogeneously, and placed in incubation jars (8.9 cm × 16.0 cm) to obtain a 5.0 cm soil depth. The sediment had a pH of 6.8, organic matter of 0.43%, P (10 N HCl), Na, K, Ca, and Mg (1N NH_4OAc, pH 7.0) of 11.84, 11.80, 9.87, 235.03 and 29.85, respectively and sum of bases of 1.5 meq/100 g. Then, the sediments were flooded with collected lake water to establish a floodwater column of 5.0 cm. The jars were then covered with aluminum foil with needle holes to prevent algae growth and prevent water loss due to evaporation. The holes maintained an ambient atmosphere in the jar headspace. The sediment-water-columns were preincubated for 12 d to equilibrate sediment oxidizing-reducing conditions.

After development of a 2-3 mm soil surface oxidized layer, KNO_3 was dissolved and applied to the overlying floodwater at a rate of 1750 mg NO_3^--N m^{-2} and 3500 mg NO_3^--N m^{-2} of added lake water, respectively. The rate of added NO_3^--N was approximated to the yearly loading rate of nitrite+nitrate for the upper portion of Breton Sound Estuary (Lane et al., 1999). Each N treatment (including control) had six replications. Three of the treatments were used to study N_2O fluxes from sediment-water-columns and NO_3^- reduction rate in overlying water over time. Another set (3) was used to quantify denitrification rate using acetylene inhibition technique. The jars were incubated at laboratory temperature (22°C). Any water in the column lost through evaporation was maintained at 5.0-cm depth by adding collected lake water.

To determine nitrous oxide emission and nitrate reduction rate, headspace gas and floodwater were sampled for N_2O and NO_3^- analyses at 0, 1, 2, 3, 5, 7, 9, 11, 13, and 16 d following the application of NO_3^-. The thickness of the aerobic soil layer was measured at the

end of the incubation period. On each sampling date, triplicate jars per treatment were sealed with gas tight caps with rubber septa. The first gas sample was collected with a plastic syringe shortly after capping, and the two more samples were collected at every two hour interval. After the third sampling, 3-ml floodwater was collected with the syringe into 20-mL glass vial. The jar was then re-opened and incubated. To determine denitrification rate, the other triplicates of each N treatment were treated with acetylene to block reduction of N_2O to N_2 (Sorensen, 1978). Immediately after the jar was closed, 10% C_2H_2 (based on the vol. of headspace) was injected into the water column. Then, the water column would be saturated with C_2H_2, and thus the sediment pore water would be filled with C_2H_2. The headspace gas samples (after sealing with lid containing septum for sampling) were collected at 0, 2, 4 and 6 hrs. After sampling, the jars were opened until the next flux measurement. Collected gas samples were immediately transferred into evacuated glass Vacutainers (vol. 10 ml) for N_2O analysis. Concentration of N_2O was carried out on a Tremitrics 9001(Austin, TX) gas chromatograph equipped with an electron capture detector at 340^oC, a Porapak Q column and a carrier gas of 5% methane in 95% Argon. Total N_2O content in the water plus gas phases was calculated using the Bunsen absorption coefficient according to the equation described by Tiedje (1982). Denitrification rate (calculated from total N_2O content in the water plus gas phases) and N_2O emission over the closure period were expressed as mg N m^{-2} d^{-1}. Collected floodwater samples were stored in the refrigerator at 4^oC until NO_3^- measurement. NO_3^- was measured on a Dionex Model 2010I Ion Chromatography System with a detection limit of 0.01 mg/l. Nitrate reduction rate was expressed in mg N m^{-2} d^{-1} and nitrate removal rate in mg N m^{-2} d^{-1}.

Results and Discussion (Big Mar)

Denitrification Rate

Denitrification rates determined by C_2H_2 blockage technique are shown in Table 1. Rates of denitrification in the control treatment were low, remaining relatively stable through the experiment, averaging 0.3 mg N m^{-2} d^{-1}. Higher denitrification rates occurred immediately after the application of NO_3^-. The rates increased with time reaching a maximum of 67.1 and 117.6 mg N m^{-2} d^{-1} on day 3 and day 5 for the 1750 and 3500-mg NO_3-N m^{-2} treatments, respectively. The rates approached the control treatment rate after 16 d incubation in the low N treatment and after 16 d incubation in the high N treatment, indicating all added nitrate had been denitrified and/or assimilated. Statistical analysis using Duncan's Multiple Range Test procedure (SAS, 1988) showed that denitrification rates were significantly (p = 0.01 level) higher in treatment receiving 3500 mg NO_3-N m^{-2} to the surface water as compared to treatment with 1750 mg NO_3-N m^{-2}. These results are consistent with the results of Lindau et al. (1994), who found in a forested wetland field study that the fluxes of labeled N_2 from the 300 kg NO_3^--N ha^{-1} treatment were significantly higher than the fluxes from the 100 kg NO_3^--N ha^{-1} rate.

Rates of denitrification determined by C_2H_2 block averaged to 57.3 and 87.1 mg N m^{-2} d^{-1} (20.8 and 31.7 g N m^{-2} yr^{-1}) over 5 d of the active period of denitrification for the 1750 and 3500-mg NO_3-N m^{-2} addition, respectively. The total N evolved as $N_2O + N_2$ over the sampling period of active denitrification was about 436.4 and 921.4 mg N m^{-2} (data not shown), corresponding to 24.9% and 26.3% of the applied NO_3^--N. The results obtained by measuring evolution of N_2O are perhaps under estimated, since several studies suggest that N_2O can be

entrapped in the soil (Lindau et al., 1988; Katyal et al., 1989) and the acetylene reduction assay tend to underestimate denitrification.

NO_3^- - Reduction Rate and NO_3^- - Removal Rate

NO_3^- concentrations in the control water column treatment remained low and changed little throughout the incubation period, ranging from 47.9 to 21.5 mg NO_3-N m^{-2}. The initial concentration of NO_3^- in the 1750 and 3500-mg NO_3-N m^{-2} treatments was 1716.0 and 3135.9 mg NO_3-N m^{-2} and was reduced to very low levels after 16 d incubation (Figure 1). Regression analysis of the NO_3^- concentrations over 16 d period indicated NO_3^- - reduction rate was found to be 84.0 and 149.9 mg NO_3-N m^{-2} d^{-1} for 1750 and 3500-mg NO_3-N m^{-2} treatments, respectively. The faster removal occurred within the earlier period and then declined gradually toward the end of incubation. The fact that maximum denitrification was found on day 3 and day 5 for the low and high N treatments (Table 1) indicates that the rapid NO_3^- reduction observed at the beginning of the experiment was a result of rapid diffusion of NO_3^- from water column into soil column and was probably immobilized by soil organisms. Denitrification may become the major pathway for NO_3^- removal with the changes and adaptation in bacterial populations to the increased NO_3^- loading. The removal rates in the high N application were significantly higher than that in the low N application during the incubation except for the first day, indicating that the higher NO_3^- concentration favors a faster NO_3^- reduction rate (DeLaune et al., 1998).
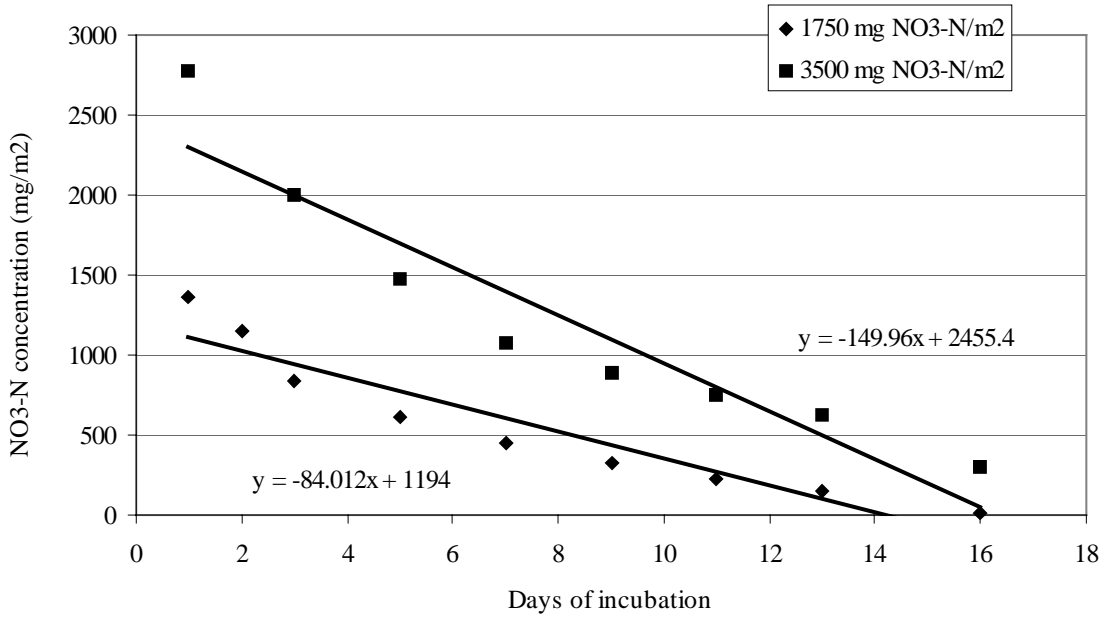
Figure 1. Changes in nitrate concentration in water column (Big Mar)

N$_2$O Emission

Figure 2 shows the rates of N$_2$O emission over time following NO$_3^-$-applications. Emission of N$_2$O from the control treatment was very low and was negative (ranged from 0 to -0.77 mg N m^{-2} d^{-1}) at most time of the sampling period. This may imply that open-water wetland ecosystems would be able to consume the atmospheric N$_2$O when mineral N is very low. The daily average N$_2$O consumption in the control was estimated to be 0.3 mg N m^{-2} d^{-1}.

The N$_2$O emission rates from both NO$_3^-$ treated sediment-water-columns increased shortly after the addition of NO$_3^-$, but with the decrease in NO$_3^-$-N pool N$_2$O emission rates declined rapidly to undetectable level after 3 and 5 days for the 1750 and 3500-mg NO$_3$-N m^{-2} treatments, respectively. Maximum emissions were recorded on day 1 (13.8 mg N m^{-2} d^{-1}) for 1750 mg NO$_3$-N m^{-2} application rate and day 2 (25.4 mg N m^{-2} d^{-1}) for 3500-mg NO$_3$-N m^{-2} rate (Figure 2). The total evolved N$_2$O –N without C$_2$H$_2$ added was calculated to be 19.2 and 51.5 mg N m^{-2} and accounting for 1.1% and 1.5% of the applied NO$_3^-$-N for the 1750 and 3500-mg NO$_3$-N m^{-2} treatments, respectively. The ratio of total N$_2$O-N evolution to the amount of NO$_3^-$-N applied to water layer was increased by 35% when the NO$_3^-$-N application rate was increased from 1750 to 3500-mg NO$_3$-N m^{-2}. This implies that if the NO$_3^-$ loading entering the wetlands would not exceed some concentration, the wetland soils may remove significant amounts of NO$_3^-$ from water by denitrification but not contribute to an appreciable amount of N$_2$O, an important greenhouse gas, emitting to the atmosphere. As much as 65% of applied NO$_3$-N was probably immobilized by soil microorganisms. The effect of NO$_3^-$ on N$_2$O emission observed in this experiment might be due to the influence of NO$_3^-$ on soil redox potential. Other studies indicate

that NO_3^- addition may buffer soil redox potential and high NO_3^- concentrations can inhibit

reduction of N_2O to N_2 (Blackmer and Bremner, 1978; Lindau and DeLaune, 1991). For other

greenhouse gases, nitrate addition primary effect in reducing methane production in soils was

through resultant increase in soil redox potential and not used in methane oxidation (Jugsujinda

et al., 1995). Concentration limit of NO_3^- to control N_2O emission should be taken into account

in future studies.

N_2/ N_2O Ratios

Denitrogen/nitrous oxide ratios (N_2/ N_2O) were calculated according to the formula

(Production N_2O+N_2 – Production N_2O)/Production N_2O for the first 3 sampling dates when

N_2O productions were significant. On the following dates when the N_2O production rates were

very low and frequently under detectable levels, the ratios were estimated using the formula

(Production N_2O+N_2 – Production N_2O)/Average Production N_2O so as to avoid drastic changes

in ratios due to measurement error. Average Production N_2O means the average of N_2O

production rates from day 5 throughout the experiment. The changes in N_2/ N_2O ratios with time

are shown in Table 2. For both 1750 and 3500-mg NO_3-N m^{-2} treatments, the ratios were low

during the first few days due to high N_2O emission rates, then increased to maximum values at

day 5 due to low daily N_2O emission. The ratios decreased again towards the end of sampling

period due to depletion of NO_3^- -N pool. Over the sampling period, evolved N_2/ N_2O ratios

ranged from 1 to 124 and 1 to 245 for the low and high NO_3^- application rates, respectively. The

highest ratios were recorded on day 3 and day 5 (Table 2). Denitrogen/nitrous oxide ratios within

the first 3 sampling dates were low for the 3500 mg N m^{-2} application rate with an average of 4

as compare to that for the 1750 mg N m^{-2} rate with an average of 43. Addition of NO_3^- has been
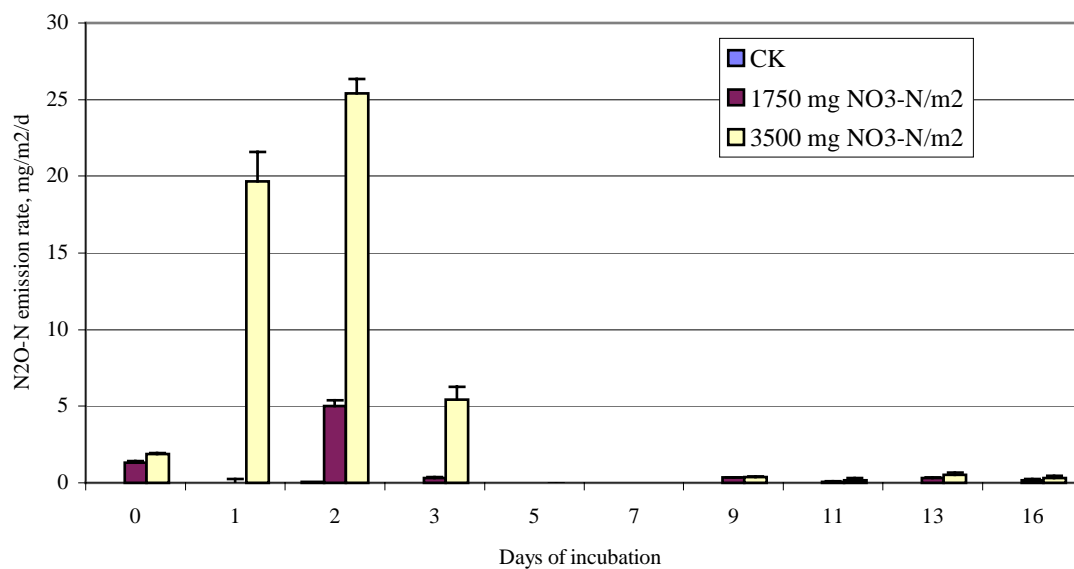
Figure 2. Nitrous oxide emission from sediment/water column (Big Mar)

shown to cause decreased soil reduction (Jugsujinda et al., 1995) and the inhibition of high NO_3^-

concentration on reduction of N_2O to N_2 (Blackmer and Bremner, 1978; Lindau and DeLaune,

1991).

Thickness of Oxidized Soil Layer

The application of NO_3^- increased the thickness of the surface oxidized soil layer (Table 3). After

16-d incubation period, the thickness of the light-brown aerobic layer was increased from 2.8 mm

of the control level to 8.2 and 13.2 mm for the low and high NO_3^- treatments, respectively. A

significant correlation between the application rate of NO_3^- and the thickness of oxidized layer

was observed (r = 0.9998, n = 3, 0.01 confidence level).

The effect of NO_3^- application on the thickness of aerobic zone is attributed to the applied

NO_3^- diffusing downward into the sediment. Generally the faster uptake of oxygen within the

bottom sediments compared to supply rate through the water column results in the development

of an oxidized surface layer and an underlying reduced layer. Thickness of the oxidized layer is

determined by the net oxygen consumption rate. It was observed that NO_3^- is present in the

surface oxidized layer, but cannot be detected in the underlying reduced layer (Reddy et al.,

1975; Reddy and Patrick, 1977). This implies NO_3^- may be consumed quickly within the reduced

zone, and hence decrease the consumption of oxygen. Reddy and Patrick (1977) found that

increasing the concentration of NH_4^+-N in the soil increased the production of NO_3^- and also the

thickness of the aerobic soil layer.

Conclusions

Anaerobic conditions existing in Big Mar sediment provides an ideal environment for reduction of nitrate-N from Mississippi River fresh water being diverted through the site. The rapid reduction of nitrate-N was found to be due to denitrification process. The rates of NO_3^- reduction (determined from change in nitrate concentration in the floodwater) averaged 84.0 mg N m^{-2} d^{-1} over 16 d for 1750 mg NO_3^--N m^{-2} addition, and 149.9 mg N m^{-2} d^{-1} over 16 d for 3500 mg NO_3^--N m^{-2} addition. The total N_2O -N emission from the 1750 and 3500 mg NO_3^--N m^{-2} additions was 19.2 and 54.1 mg N m^{-2} accounting for 1.1% and 1.5% of the applied NO_3^--N, respectively. Using the acetylene blockage technique, average denitrification rate was determined to be 57.3 and 87.1 mg N m^{-2} d^{-1} (20.8 and 31.7 g N m^{-2} yr^{-1}) during active denitrification period of 5 days after incubation for 1750 and 3500 mg NO_3^--N m^{-2} of added nitrate in floodwater, respectively. The total N evolved as $N_2O + N_2$ was about 436.4 and 921.4 mg N m^{-2} (24.9% and 26.3%, respectively of added N). Increasing the amount of NO_3^- applied to the overlying water increased rate of NO_3^- loss and N_2O emission. The thickness of the oxidized surface soil layer was also influenced by the NO_3^- application rate to the floodwater with a significant linear correlation between nitrate addition and thickness of the oxidized layer (r = 0.9998, P = 0.01). Lane (1999) found loading rate of nitrite + nitrate of 5.6-13.4 g N m^{-2} yr^{-1} as diverted Mississippi River water entered the estuary. Our study suggests that Big Mar and other wetlands in upper Breton Sound Estuary have the capacity to process significant quantity of nitrate, thus lowering and reducing nitrate level in coastal region in the lower estuary. The results show denitrification, assimilation and/or immobilization are significant NO_3^-N removal processes.

TABLE 1. Denitrification rate (Big Mar) following addition of low and high rates of NO_3-N with C_2H_2.

	Denitrification rate (mg N/m$_2$/d)											
Treatment	Days of incubation											
(with C_2H_2)	0	1	2	3	5	7	9	11	13	16	Total	Average
CK	0.44	0.00	0.95	0.56	0.28	0.02	0.38	0.03	0.22	0.00	2.46	0.27
	(0.10)	(0.00)	(0.17)	(0.07)	(0.03)	(0.08)	(0.04)	(0.00)	(0.05)	(0.00)		
1750 mg NO$_3$-N/m$_2$	9.99	53.49	60.71	67.08	48.22	37.90	16.07	4.60	1.27	-0.16	289.22	32.13
	(1.31)	(5.34)	(7.37)	(17.93)	(7.59)	(7.68)	(5.54)	(2.31)	(0.45)	(0.07)		
3500 mg NO$_3$-N/m$_2$	14.1	53.60	67.04	110.43	117.59	83.54	48.19	18.54	33.64	8.78	541.39	60.15
	(0.75)	(2.32)	(7.51)	(14.79)	(2.20)	(10.93)	(0.78)	(6.51)	(10.20)	(8.26)		

Note: Data are mean with standard error in parentheses, n=3

TABLE 2. N_2/N_2O ratio in sediment water column (Big Mar) following the addition of low and high rate of NO_3-N.

	N_2/N_2O ratio											
Treatment	Days of incubation											
	0	1	2	3	5	7	9	11	13	16	Total	Average
1750 mg NO$_3$-N/m$_2$	4	1	6	124	103	79	32	9	2	-1	356.33	39.59
3500 mg NO$_3$-N/m$_2$	4	1	1	11	245	175	99	38	68	17	655.56	72.84

TABLE 3. Thickness of oxidized sediment layer (Big Mar) following addition of low and high rate of NO_3-N after 16 d incubation.

Treatments	Rep 1	Rep 2	Rep 3	Average	Standard deviation
	(mm)	(mm)	(mm)	(mm)	
CK	3	2.5	3	2.8	0.29
1750 mg NO$_3$-N/m$_2$	8	8.5	8	8.2	0.29
3500 mg NO$_3$-N/m$_2$	13.5	13	13	13.2	0.29

Site B-Davis Pond (Lake Cataouatche)

The Davis Pond freshwater diversion structure is located on the west bank of the Mississippi River above New Orleans near Davis, LA, at river mile 18. The structure is designated to disperse freshwater and accompanying sediments from the Mississippi River into Barataria Basin to combat saltwater intrusion and land loss, which will help mitigate the effects of subsidence.

The Davis Pond project is scheduled to be operational in Summer 2001. The structure will be capable of introducing up to 10,000 cfs of freshwater into Barataria Basin. Actual discharge rates, based on a parallel freshwater diversion project (Caernarvon), will likely be on the order of 1,000 to 2,000 cfs. The inflow will be allowed to seek its course through a 20 to 25 square mile levied freshwater marsh before discharging into Lake Cataouatche. Denitrification potential of sediment from Lake Cataouatche, the receiving body for Mississippi River water at the Davis Pond Freshwater Diversion was also studied. This dentrification study objectives were:

1) to quantify the emission of dinitrogen and nitrous oxide to the atmosphere resulting from dentrification,

2) to quantify the differences in external loading and internal loading contributions to nitrogen gas flux,

3) to quantify the nitrogen processing capacity,

4) to verify the acetylene inhibition technique with the ^{15}N isotope technique, and

5) to identify implications of the impacts the diversion may have on the receiving basin.

We hypothesized that this sediment has a large potential for dentrification and nitrogen assimilation, and may reduce nitrate transport into lower Barataria Basin Estuary. Dentrification in Lake Cataouatche sediment was measured twice using the acetylene inhibition technique (September 15, 2000/December 14, 2000) and once using the ^{15}N isotope method (November 22, 2000). In both fall and winter experiments, samples were collected from the same location in the lake (Latitude 29.8227 N, Longitude 89.92175 W). Samples were collected from the top 15 cm of sediment using a Peterson dredge from three sites in the immediate vicinity of the coordinates. Sediment was transported in lined containers to the laboratory where it was mixed to achieve homogeneity. All large debris and mollusks were removed. This preparation of sediment was intended to homogenize the sediment and minimize hot-spots of dentrification often occurring in natural conditions.

For all experiments, the sediment was added to incubation jars (8.9 cm x 16.0 cm) to obtain a depth of 5 cm, and flooded with 5 cm of lake water. All incubation jars were wrapped in aluminum foil with needle holes to prevent algae growth and limit loss of water through evaporation. The jars were incubated in the dark (ambient laboratory temperature 22° C) for about two weeks, to allow the formation of an oxidized layer at the surface, which indicated the development of oxidized-reduced conditions.

The acetylene inhibition technique was employed in September and December experiments. The technique allows the indirect measurement of dentrification by blocking the final enzyme catalyzed step of nitrate reduction from nitrous oxide to dinitrogen gas with acetylene gas, limiting the major end products to nitrous oxide (Sorensen, 1978). The flux of nitrous oxide from the sediment representing the combined fractions of N_2O and N_2, the primary end products of dentrification, can easily be determined with gas chromatography. Two sets of

incubation jars were amended with dissolved potassium nitrate (KNO_3) to achieve 0, 1.4 and 50

mg-NO_3-N/l concentrations. The nitrate concentrations represent an experimental control, a low

nitrate concentration to mimic the nitrate level in the Mississippi River at New Orleans, and a

high nitrate concentration to elicit the denitrification potential. Of the two sets of incubation jars,

one was used as a control set, while the second was treated with acetylene gas. Furthermore, in

each set, three replicate jars were used for each of the three nitrate concentrations.

The incubation jars were sealed at the start of each sampling period with gas tight caps

with rubber septa. Prior to acetylene injection, headspace air was removed from the second set to

create a slight vacuum, which allowed the injection of an equal volume of acetylene without

overpressure in the headspace. Acetylene gas, injected at 10% of the headspace volume, was

slowly injected into the floodwater before each sampling period and allowed to diffuse into the

sediment for 90 min. Flux measurements of nitrous oxide were taken from closed jars using a 2-

ml syringe at 90, 120, 180, and 240 min after incubation jars were sealed. The jars were open to

the atmosphere after the sampling periods to allow natural gas exchange within the floodwater

and sediment. Sampling occurred over the course of 24 days on day 1, 3, 5, 7, 10, 13, 16, 20, and

24 after the sampling sets were amended with KNO_3.

The gas samples were immediately analyzed using a Shimadzu GC-14A Gas

Chromatograph fitted with a 2-ml sampling loop, Poropak Q 1.8 m column, and electron capture

detector. The instrument used a carrier gas of ultra high pure nitrogen and operated at

temperatures of 40, 100, and 290° C for oven, injector, and detector, respectively. Rates of

dentrification were determined by the linear regression of gas flux, corrected with the Bunsen

absorption coefficient (Tiedje, 1982) to estimate total N_2O. Nitrous oxide flux was estimated

using the closed chamber equation by Rolston (1986):

$$F = (V/A)(273/T)(\Delta C/\Delta T),$$

Where V is the headspace volume in the jar, A is the sediment surface area of the jar, T is the absolute temperature of the headspace gases, and $\Delta C/\Delta T$ is the change in concentration of N_2O per unit of time. Nitrous oxide flux is reported in mg-N/m^2-d.

Concurrent with gas flux sampling, 2 ml samples of floodwater were removed from each jar on each sampling day for nitrate analysis. Water samples were collected in glass vials and stored in a refrigerator until analysis. Water samples were analyzed with a Spectronic Genesys 5 UV spectrophotometer at a wavelength of 220 nm and corrected with twice the absorption at 275 nm for dissolved organic matter (Standard Methods). Results of N_2O emission were compared to the rate of decrease of nitrate in the overlying floodwater.

The ^{15}N technique allowed the direct measurement of ^{15}N flux from the sediment cores. Two replicate pre-incubated jars were amended with 56.6 atom % labeled ^{15}N nitrate to achieve a final concentration of 50 mg-NO_3-N/l. Sampling of the headspace gas occurred after 24 h periods, with the jars sealed, using a 20 ml syringe. Headspace gas samples were transferred into 10 ml Vacutainers and stored until analyzed. Sampling occurred on days 2, 4, 6, 8, 10, 13, 15, 17, 19, 21, 23, 25, 27, and 29 from the initial amendment of nitrate. Lids were removed for days when sampling did not occur. After a run of 29 days, the regular sampling was discontinued and the sediment was analyzed for entrapped gases. Both jars were sealed and shaken vigorously by hand to release entrapped gases and headspace gas was sampled immediately.

Gas samples containing labeled ^{15}N nitrate were analyzed with a Finnigan Mat Delta Plus gas isotope ratio mass spectrophotometer. Emissions were calculated using the equations of Mulvaney and Boast (1986).

Results

Nitrate Removal (Davis Pond)

Nitrate removal from the overlying floodwater following KNO_3 amendments were consistent among replicates and showed similar patterns for both studies in September and December. Removal rates were estimated from a linear regression of specific segments of the removal curve where major rate changes were observed graphically (Figure 3). The corresponding time intervals occurred from days 1 to 9 and from days 9 until sampling ended. R^2 values (0.78 - .99) suggest a good fit for each regressed interval.

The removal rate was an exponential decrease for the two treatments (initial concentrations of approximately 1.4 mg l^{-1} and 50 mg l^{-1}) and no significant changes for controls. The rapid initial decrease under low loading (1.4 mg l^{-1}) occurred until day 9 at approximately 10 mg N m^{-2} d^{-1}, removing nearly all of the nitrate from the water column (Figure 4). Subsequent rates decreased to less than 1 mg N m^{-2} d^{-1} until sampling was terminated after 16 days. Final nitrate concentration for the low nitrate treatment approached that of the controls at approximately 0.3 mg l^{-1}. The removal of nitrate in high nitrate treatments (50 mg l^{-1}) was initially ten-fold higher that the low nitrate treatment, achieving rates between 157 and 167 mg N m^{-2} d^{-1} from day 9 until day 24 (Figure 5). The samples at day 24 for the high nitrate treatment had a final concentration of less than 5 mg NO_3-N l^{-1}.

Acetylene Inhibition Technique

Denitrification rate of sediment treated with acetylene showed similar patterns for each treatment of the two studies, where N_2O emissions increased to a peak then fell slightly to a wavering rate that persisted until the termination of the experiment (Figure 6 and 7).
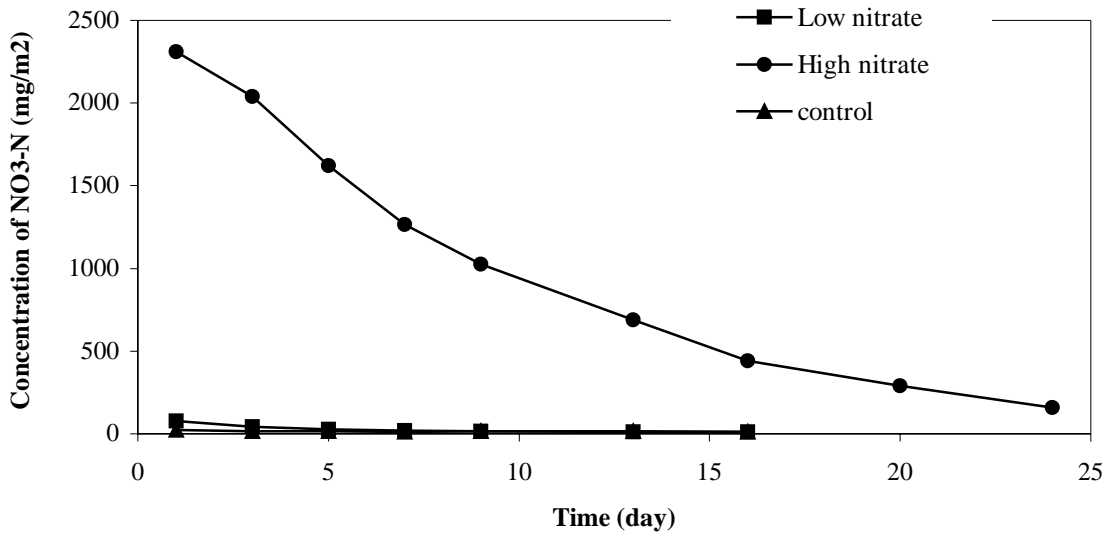
Figure 3. Removal of nitrate in the overlying flood water of sediment cores from Lake Cataouatche (September).
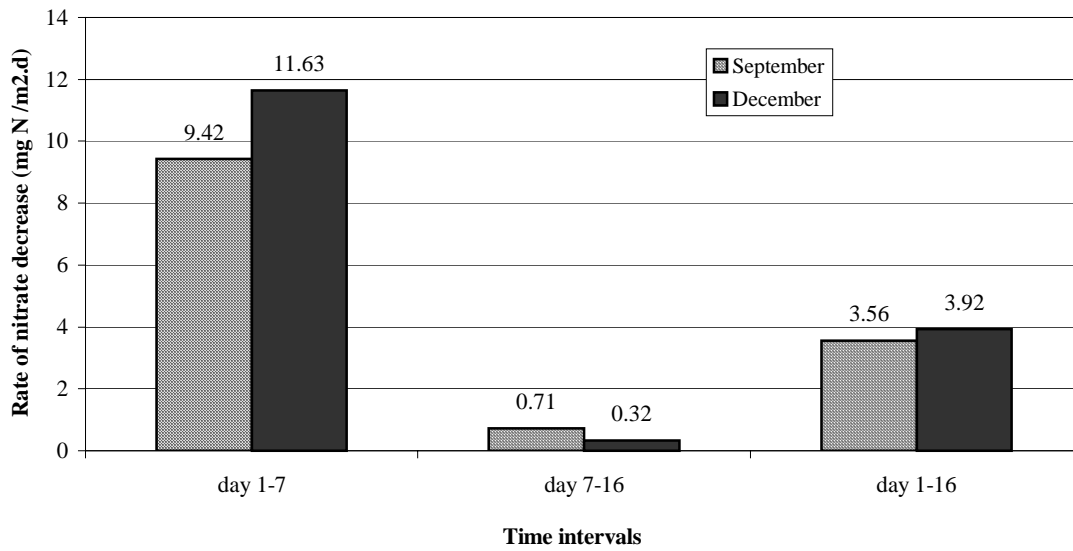
Figure 4. Rate of Nitrate disappearance in floodwater of Lake Cataouatche sediment
incubation jars with initial concentration of 1.4 mg NO3-N/l
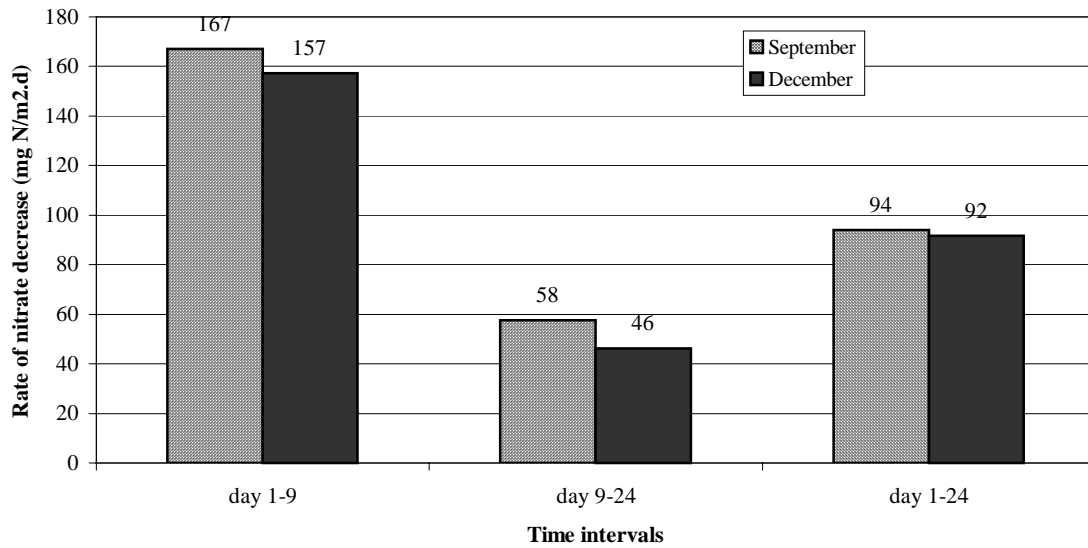
Figure 5. Rate of Nitrate disappearance in floodwater of Lake Cataoutche sediment
incubation jars with initial conentration of 50 mg NO3-N/l
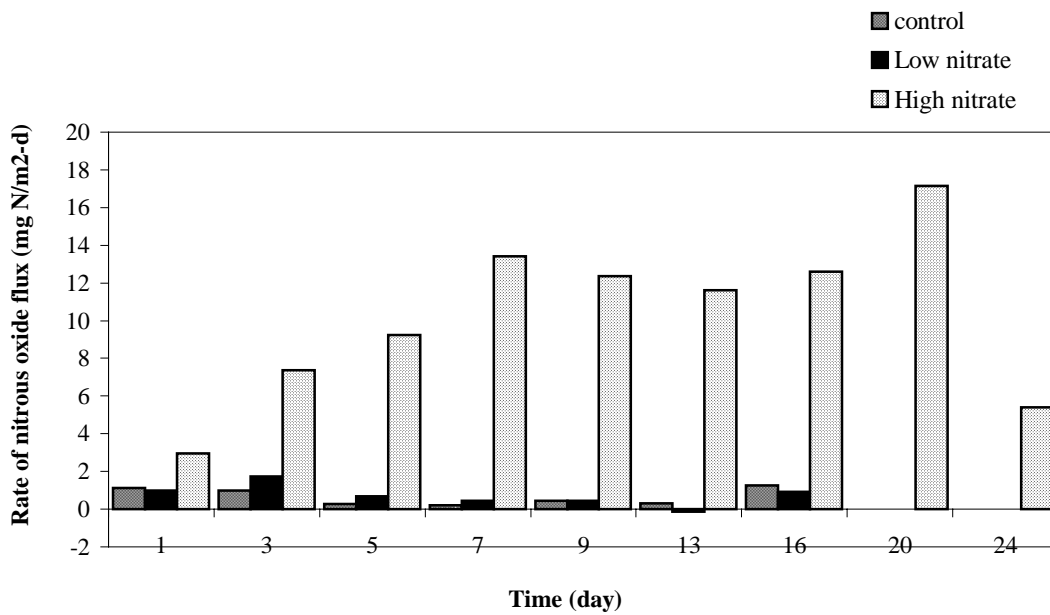
Figure 6. Nitrous oxide flux from Lake Cataouatche sediment cores with acetylene treatment (September).
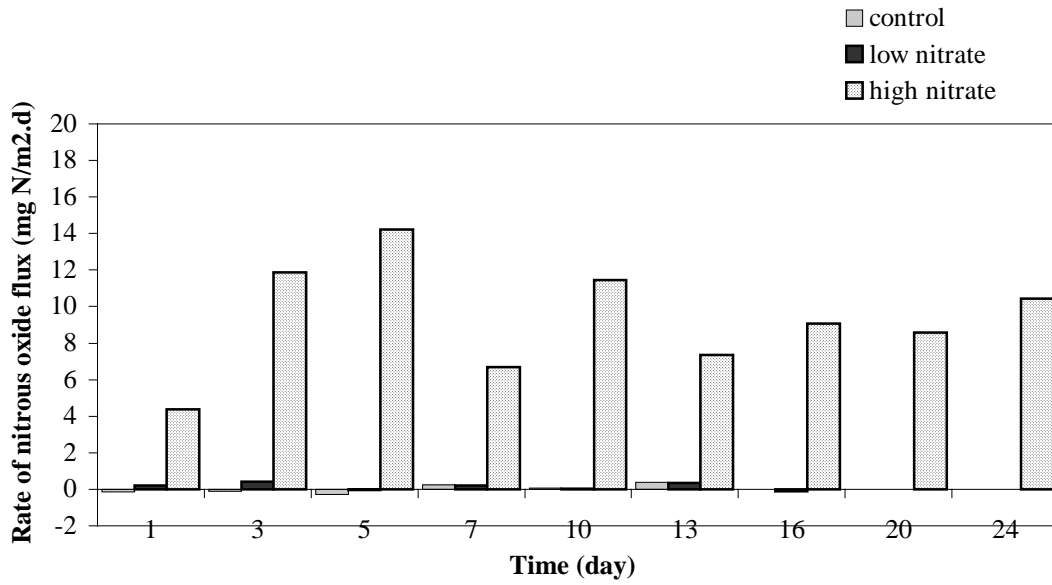
Figure 7. Nitrous oxide flux from Lake Cataouatche sediment cores with acetylene treatment (December)

Denitrification rates achieved a maximum of 1.74 and 0.40 mg m^{-2} d^{-1} for low nitrate treatments

at day 3 in fall and winter, respectively. For high nitrate treatments, a peak at day 7 of 13.4 mg N

m^{-2} d^{-1} was observed for the fall study, and a maximum of 14.2 mg m^{-2} d^{-1} was reached in winter.

15 N Isotope Technique

Total N flux (^{14}N and ^{15}N) from sediment cores was determined by multiplying direct

measurements of N_2O+N_2-^{15}N emission from the cores with a factor of 3.1541 determined from a

ratio of estimates of total N flux and ^{15}N flux in two samples. Denitrification rates compared

favorably to results from the acetylene treatment, showing a rapid increase to a maximum of 10.8

mg N m^{-2} d^{-1} at day 6 and declining until the end of the experiment (Figure 8). Results, however,

showed two anomalous values, 1.7 and 1.2 mg N m^{-2} d^{-1} for day 13 and day 21, respectively, that

may have been caused by sampling or instrument error.

The N_2O+N_2 entrapment study revealed that a significant fraction of N_2O+N_2 remained in

the sediment pore water. Total entrapped N_2O+N_2-^{15}N determined at the end of the experiment

was uniformly distributed among each of the sample measurements, more than doubling initial

N_2O-^{15}N flux measurements. Peak height of the denitrification rate curve increased from 3.4 mg

N m^{-2} d^{-1} to 8.0 mg m^{-2} d^{-1}.

Conclusion

Denitrification potential was determined for sediments of Lake Cataouatche with the

aceytlene inhibition technique and verified with the 15N isotope technique. Maximum

denitrificaion rates were achieved with high nitrate amendments and the acetylene inhibition

technique at day 7 and 5 for fall and winter experiments reaching 13.4 and 14.2 mg N m^{-2} d^{-1},

respectively. The initial increase in nitrous oxide emission was followed by a sustained flux of

gas after peak levels were reached. Results from the isotope technique compares favorably to the

acetylene technique, showing a similar trend through the duration of the experiment and achieving a peak of 10.8 mg N m^{-2} d^{-1}.

The denitrification potential exceeded the denitrification rate under low nitrate amendments by approximately ten times. As this low nitrate concentration (1.4 mg NO_3-N l^{-1}), which simulates nitrate levels in the Mississippi River water, it is concluded that the sediment of Lake Cataouatche has the capacity to denitrify additional inputs of nitrate, beyond the typical load in the Mississippi River at New Orleans. This sediment also has the potential to remove nitrate in the overlying water down to 0.3 mg NO_3-N l^{-1}, values comparable to experimental controls under laboratory conditions.

Nitrate removal from the overlying floodwater followed an exponential decline that persisted until the end of the experiment. The denitrification potential is approximately 10% of the nitrate removal over the first 7-9 days of the experiment (157 and 167 mg N m^{-2} d^{-1}). Denitrification rates under low nitrate amendments similarly follow initial nitrate removal rates at approximately 10%. Following the rapid decrease in nitrate, denitrification efficiency greatly improves and is sustained. This trend may be due in part by several factors. An initial increase in microbial population or the reduction in denitrifying enzymes in the sediment stimulated by the addition of nitrate may account for the assimilation of the nitrate pool. The simultaneous reduction of nitrate to ammonium and the subsequent nitrification and denitrification of ammonium competes with the denitrification process. Coupled with increases in the oxidized layer, which allows greater internal contributions of nitrate to denitrification, a sustained rate of denitrification can be supported in the sediment.

Results demonstrated that the system has a large potential for denitrification and nitrate assimilation or immobilization. Lake Cataouatche sediments thus should significantly decrease the movement of nitrate into the lower estuary and reduce risks for eutrophication.
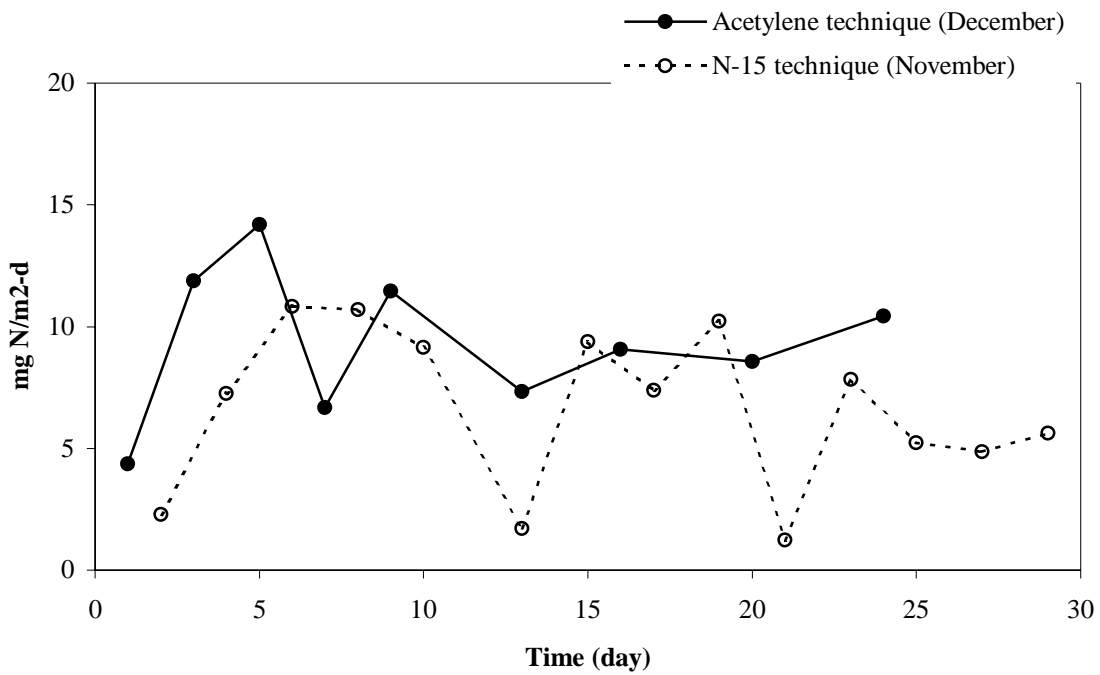
Figure 8. Comparison of denitrification rates with acetylene inhibition and N-15 techniques in high nitrate treated sediment cores from Lake Cataouatche.

References

1. Antweiler, R.C., D.A. Goolsby and H.E. Taylor. 1995. Nutrients in the Mississippi River. *In* Contaminants in the Mississippi River. 1987-92. Robert H. Meade Editor, U.S. Geology Survey Circular. 1133, 140 p.

2. Blackmer, A.M. and J.M Bremner. 1978. Inhibitory effect of nitrate on reduction of N_2O to N2 by soil microorganisms. Soil Biology and Biochemistry. 10: 187-191.

3. DeLaune, R.D., C.W. Lindau, E. Sulaeman and A. Jugsujinda. 1998. Nitrification and denitrification estimates in a Louisiana swamp forest soil as assessed by ^{15}N isotope dilution and direct gaseous measurements. Water, Air and Soil Pollution. 106: 149-161.

4. Jugsujinda, A., R.D. DeLaune and C.W. Lindau. 1995. Influence of nitrate on methane production and oxidation in flooded soil. Commun. Soil Sci. Plant Anal. 26:2449-2459.

5. Katyal, J.C., L.S. Holt and A.M. Gadalla. 1989. A method to determine soil-entrapped denitrification products in submerged soils. Journal of the Soil Science Society of America. 53: 296-297.

6. Lindau, C.W. and R.D. DeLaune. 1991. Dinitrogen and nitrous oxide emission and entrapment in *Spartina alterniflora* saltmarsh soils following additon of N-15 labeled ammonium and nitrate. Estuarine, Coastal and Shelf Science. 32: 161-172.

7. Lane, R.L., John W. Day, Jr. and Nurnell Thibodeaux. 1999. Water quality analysis of a freshwater diversion at Caernarvon, Louisiana. Estuaries 22:327-336.

8. Lindau, C.W., R.D. DeLaune and J.H. Pardue. 1994. Inorganic nitrogen processing and assimilation in a forested wetland. Hydrobiologia. 277: 171-178.

9. Lindau, C.W., W.H. Patrick, Jr., R.D. DeLaune, K.R. Reddy and P.K. Bollick. 1988. Entrapment of nitrogen-15 dinitrogen during soil denitrification. Journal of the Soil Science Society of America. 52: 538-540.

10. Reddy, K.R. and W.H. Patrick, Jr. 1977. Effect of placement and concentration of applied NH_4^+-N on nitrogen loss from flooded soil. Soil Science. 123: 142-148.

11. Reddy, K.R., W.H. Patrick, Jr., and R.E. Phillips. 1976. Ammonium diffusion as a factor in nitrogen loss from flooded soil. Soil Sci. Soc. Amer. Proc. 40: 528-533.

12. Ryden, J.C. and D.E. Rolston. 1983. The measurement of denitrificatioon. In: Freney, J.R. and J.R. Simpson, eds. Gaseous loss of nitrogen from plant–soil systems. Martinus Nijhoff Dr W. Junk Publishers, The Hague: 91-132.

13. SAS Institute. 1988. SAS STAT User's Guide. Release 6.23 Edition. SAS Institute Inc., Cary N.C.

14. Smith, C.J., R.D. DeLaune and W.H. Patrick, Jr. 1983. Nitrous oxide emission from Gulf Wetlands. GEOCHIMICA ET COSMOCHIMICA ACTA. 47: 1805-1814.

15. Sorensen, J. 1978. Denitrification rates in a marine sediment as measured by the acetylene inhibition technique. Appl. Environ. Microbiol. 36: 139-143.

16. Tiedje, J.M. 1982. Denitrification. P.1011-1026. In: A.L. Page, R.H. Miller and D.R. Keeney (eds.) Methods of Soil Analysis, Part2. Chemical and Microbiological Properties (2nd ed.).

17. Turner, R.E. and N.N. Rabalais. 1994. Coastal eutrophication near the Mississippi River Delta. Nature 368:619-621.

Basic Information

Title:	Quantifying Urban Non-Point Sources of Lead for use in TMDL Computations
Project Number:	GR02673 C-04 FY00
Start Date:	3/1/2000
End Date:	2/28/2001
Research Category:	Water Quality
Focus Category:	Non Point Pollution, Water Quality, Management and Planning
Descriptors:	Lead, roof runoff, urban runoff, non-point source pollution, total maximum daily load, TMDL
Lead Institute:	Louisiana Water Resources Research Institute
Principal Investigators:	Laura J. Steinberg

Publication

Quantifying Urban Non-point Sources of Lead for use in TMDL Computations

Dr. Laura J. Steinberg – *Assistant Professor, Tulane University Department of Civil and Environmental Engineering*

Ridgely P. Myers – *Graduate Student, Tulane University Department of Civil and Environmental Engineering*

OBJECTIVES

Louisiana has designated 104,248 acres of lakes and 2,475 miles of rivers and streams as being environmentally degraded due to lead contamination (Louisiana Department of Environmental Quality, 1998). In the development of total maximum daily loads (TMDLs), as mandated by the Clean Water Act, the state must set maximum limits for the discharge of pollutants, accounting for the non-point sources of contaminants. Recent evidence has indicated that two sources may be contributing to non-point source loadings of lead, yet the effect of these sources on water quality has not been adequately determined. These sources of lead are rain runoff from rooftops and rain runoff from the exterior walls of structures painted with lead-based paint, which was used up to 1978. These sources were investigated in this project.

Numerous publications have documented the presence of lead in urban runoff (Ellis, 1977; Whipple and Hunter, 1981; USEPA, 1983; Cole et al., 1984; Flores-Rodriguez et al., 1993; Martin, 1995; Tsihrintzis and Hamid, 1998). Much of this lead is attributed to road and highway runoff (Kerri, 1985). The use of leaded gasoline up to 1985 made this a very significant source. However, recent studies have indicated that residential homes may also be important sources of urban lead pollution. These studies are of particular significance in New Orleans, where Mielke et al. (1999) has demonstrated that much of the top-soil has lead concentrations of more than 300 µg/l, and that there are sections of the city with soil concentrations as high as 1100 µg/l. Mielke also noted that the largest concentrations of lead were found at the base of the exterior walls.

A study by Ni, et al. (1995) indicated brick and wood buildings, and possibly building roofs, as major contributing sources of lead to urban storm water runoff. Paints produced from 1884 to 1978 characteristically had very high lead content and remains on the walls of many older structures (Mielke et al., 1999). This lead is thought to be mobilized by rainfall. Additionally, paint collected on adjacent soils due to natural or forced removal of the paint may act as a lead source (Davis and Burns, 1999).

Yaziz et al. (1989) studied lead concentrations emanating from tile and galvanized iron roofs in Malaysia. He found average levels of "first flush" lead in the roof runoff of 235 µg/l for the galvanized iron roof and 102 µg/l for the tile roof. Good (1993) studied roof runoff lead concentrations at a Washington state sawmill, whose runoff flows directly to into a nearby water body. He found that heavy metal concentrations of copper, lead, and zinc all exceeded the EPA standards for discharge into marine waters. Sampling was done at several different types of rooftops, including galvanized metal, roofing paper and

tar, and anodized aluminum. Even the tar roof, which was not expected to contain any lead in its constituent material, produced unacceptably high concentrations of lead. Good collected samples at the beginning of the rain event, and then again three hours later. He found that the metal concentrations were generally lower after the "first flush" and theorized that this resulted from the early removal of easily dislodged particles containing metals.

Davis and Burns (1999) measured concentrations of lead in roof runoff in Prince George County, Maryland. They found mean levels of lead in the runoff from rooftops of 38 µg/l with a standard deviation of 110 µg/l. The type of roofing material was not specified. Their work was motivated by a monitoring study of heavy metals in urban runoff performed by Ni et al. (1995) in Prince George County, Maryland. They studied the lead concentration in runoff from exterior, painted walls by spraying them with synthetic rainwater. They found concentrations of total lead as high as 28,000 µg/l for surfaces with paint older than 10 years. For this type of paint, the mean value of the concentration was 810 µg/l. Newer paint, 0-5 years old, produced maximum lead concentrations of 370 µg/l and a mean concentration of 27 µg/l. The authors attribute the difference between these two sets of runoff to the fact that older paint is more likely to contain high amounts of lead, and older paint is likely to peel more easily, thus yielding more particulate lead. Furthermore, the researchers found that an increase in the intensity of the spray increased the concentrations of lead measured in the runoff.

As shown, there is emerging evidence that wall runoff from surfaces with leaded paint is an important source of lead in urban runoff. In addition, some evidence exists that rooftops may store lead particles and release them in particulate or dissolved form during rainfall events.

METHODS

The selection of homes for the study was based on the existence of leaded paint on the exterior walls. Paint chips were collected from homes in New Orleans located in neighborhoods previously identified as having high levels of lead in the soils (Mielke et al., 1999). Loose, peeling paint chips from 30 homes were removed and transported to the laboratory in wide-mouthed 200 ml polyethylene bottles preconditioned with a 1:6 ratio of hydrochloric acid and deionized water.

Acid digestion of the chips was performed in a CEM microwave. Prior to placement in the microwave vessel, a 0.5 g sample was cut from the chip and placed in 10 ml of HNO_3. Micro-waving proceeded in 4 stages, with pressure increasing from 20 psi to 80 psi. Following complete digestion, the samples were transferred to the ICP-AES for lead analysis.

A sample of 10 homes, eight with high lead content (greater than 10,000 ppm), one with medium lead content (600-10,000 ppm), and one with low lead content (less than 600 ppm), from the exterior paint sample was retained for the study. The roofing materials of the chosen houses are identified below:

House Number	Roofing Material
1	asbestos shingle (low lead content)
2	asbestos shingle
3	tar paper shingle
4	asbestos shingle
5	asbestos shingle
6	asbestos shingle
7	asbestos shingle
8	tar paper shingle
9	tar paper shingle
10	slate

Four homes were outfitted at the base of a gutter downspout with a collection device consisting of three 200 ml polyethylene bottles connected by ¾" PVC piping. Each sample bottle contains a ping-pong ball which blocks the opening of the bottle once it has filled up. (See Figure 1 to view the collection assembly) In this way, rooftop runoff was collected for the "first flush" and then for two distinct periods afterwards. The lengths of these periods depend on the rainfall intensity and the amount of roof area that drains into the rain gutter used for sampling.

The sample bottles were preconditioned with a 1:6 ratio of hydrochloric acid and deionized water. Immediately prior to each rain event, the collection devices were placed at each sample house. Typically, three to four houses were sampled during each event.

In addition to the four homes at which samples were collected from the in-place metal gutters, three homes were outfitted with preconditioned PVC rain gutters. The use of the artificial PVC gutters ensures that all lead in the samples comes from rooftop drainage, rather than from the metal gutters. The downspout from the PVC gutters consisted of vinyl tubing. (See Figure 2 to view the artificial PVC gutter) Three samples were collected from the PVC gutter during each rain event in the same way that the samples from the in-place metal gutters were taken. (See Figure 3 to view the installation of the PVC gutter.)

Three homes from the ten homes identified earlier were identified for wall runoff sampling during each rain event. Of these three homes, one each is of high, medium, and low lead content, as identified by the paint chip samples. Preconditioned plastic troughs were placed at the base of the exterior wall during the rain event, and approximately 50 ml of rainwater was collected for each sample. The water was immediately transferred to preconditioned polyethylene bottles.

Immediately after collection of roof or wall runoff, the samples were measured to determine pH. A portion of each sample was then filtered through a 0.2-micron syringe filter. Both samples were acidified with sufficient hydrochloric acid to reduce the pH of the sample to 2 or below. The acidification aids in dissolving all of the lead particles into solution. Particulate lead concentration was quantified by subtracting the total lead value

of the unfiltered portion from the lead concentration in the filtered portion. After acidification, the samples were stored at 4ºC until lead analysis was performed.

Lead analysis was initially performed in the ICP-AES, a Perkin Elmer Optima 3000. Samples that measured very small levels of lead in the ICP-AES were identified and further analyzed in a GFAA for more accurate readings. The GFAA is a Perkin Elmer 4100. Analysis occurred at Tulane University's Coordinated Instrumentation Facility, which is a department operating under the Tulane Office of Research for the management of shared research equipment.

The greatest obstacle in this research resulted from the lack of rainfall in the New Orleans area in the year 2000. The year 2000 was the driest on record for New Orleans, with only 38.88 inches of precipitation during the course of the year (*The Times-Picayune,* January 2, 2001). The year 2001 did not offer any relief either, as the drought has continued. The precipitation total for the Greater New Orleans area as of May 27, 2001 for this year is 15.62 inches, whereas the normal year-to-date precipitation is 24.20 inches (*The Times-Picayune,* May 27, 2001). Furthermore, the Gulf Coast area often experiences widely scattered showers, making it difficult to locate rainfall in the specific location of the houses chosen for analysis. These houses are also located in inner-city urban neighborhoods, so it was not feasible to collect samples from rain events that occurred or began late in the evening. However, the Principal Investigator is continuing the study beyond the USGS project completion date, and will collect additional roof and wall runoff samples as rain events occur in New Orleans during the spring and summer of 2001.

Due to the lack of rainfall events during the course of the project, the investigators opted to create synthetic rain water to gather additional data. The synthetic rain water was synthesized as 77µM NaCl, 3.8 µM H_2SO_4, and 3 µM HNO_3 in deionized water. This synthetic rain water had a pH of 5.6-5.8, typical of natural rain water in New Orleans, as determined from previous sampling data. The synthetic rain water was applied to the rooftop from a bucket via a pump at a rate of 3.2 gal/hr. As it exited the pump tubing, it passed through a 90º full-cone PVDF spray nozzle with a 0.053-inch orifice (Cole-Parmer). Each portion of the roof was washed for approximately 20 minutes, and the first flush was collected, as well as two distinct periods afterwards. (See Figures 4 and 5 to view pictures taken during sample collection with the PVC gutter using synthetic rain water.) The collection method was the same for the synthetic rainfall events as it was for the natural rain events, as discussed above.

RESULTS

The amount of lead present in the paint chips collected from the 30 homes sampled is shown below. The shaded cells represent those houses chosen for further investigation.

Table 1: Paint Chip Results

House Number	Lead (ppm)	House Number	Lead (ppm)
1	567	16	4182
2	78725	17	3177
3	8186	18	4613
4	22583	19	3353
5	99480	20	7848
6	22554	21	5588
7	61584	22	1145
8	11881	23	1885
9	38530	24	136
10	39121	25	361
11	34000	26	1080
12	20180	27	11547
13	error	28	6879
14	error	29	8352
15	15425	30	21549

Table 2, below, shows the results from samples collected for each rain event. The first two rain events gathered were natural rainfalls, and the third set of data is results from synthetic rain water. The house numbers are indicated, which may be used to reference Table 1, above. The sample location represents wall or roof runoff; however, few wall samples have been gathered to date. For the third collection date, samples were taken from the natural gutters as well as using the artificial PVC gutters. For those samples where the PVC gutters were used, this is indicated under "Sample Location." The collection sequence indicates the sample time in reference to the time lapsed during the rain event. The first flush is indicated by "1," and generally occurs during the first five minutes of the rain event. The second collection (collection sequence "2") takes place 5-10 minutes from the start of the rainfall, and the third collection (collection sequence "3") occurs approximately 10-20 minutes after the start of the rainfall. The samples that were filtered are also indicated, followed by the lead concentration in ppm (mg/l).

Samples from the second collection event which showed low concentrations after ISP-AES analysis were re-analyzed on the GFAA. These measurements are indicated by an asterick (*). The GFAA was unavailable for further analysis of the third collection event runoff samples. This analysis will take place at a later date.

Table 2: Rain Collection Data

	House Number	Sample Location	Collection Sequence	Filtered	Lead (ppm)	
Collection # 1 – Natural Rain						
	1	wall	n/a		1.202	
	2	wall	n/a		1.492	
	1	roof	3		0.000	
	2	roof	1		0.596	
	5	roof	3		0.000	
	8	roof	1		0.078	
Collection # 2 – Natural Rain						
	Pure Rain	n/a	n/a		0.003	*
	Pure Rain	n/a	n/a	x	0.000	*
	2	roof	1		0.112	*
	2	roof	1	x	0.006	*
	2	roof	2		0.015	*
	2	roof	2	x	0.000	*
	2	roof	3		0.216	*
	2	roof	3	x	0.007	*
	4	roof	1		0.013	*
	4	roof	1	x	0.000	*
	4	roof	2		0.000	*
	4	roof	2	x	0.000	*
	8	roof	1		0.041	*
	8	roof	1	x	0.002	*
	8	roof	2		0.389	
	8	roof	2	x	0.000	*
	8	roof	3		0.003	*
	8	roof	3	x	0.000	*
Collection # 3 – Synthetic Rain Water						
	1	roof	1		0.930	
	1	roof	1	x	0.472	
	1	roof	2		0.272	
	1	roof	2	x	0.147	
	1	roof	3		0.206	
	1	roof	3	x	0.124	
	1	roof (PVC)	1		0.177	
	1	roof (PVC)	1	x	0.005	
	1	roof (PVC)	2		0.340	
	1	roof (PVC)	2	x	0.004	
	1	roof (PVC)	3		0.009	
	1	roof (PVC)	3	x	0.009	
	2	roof	1		11.708	
	2	roof	1	x	0.004	

	House Number	Sample Location	Collection Sequence	Filtered	Lead (ppm)
	2	roof	2		2.662
	2	roof	2	x	0.005
	2	roof	3		6.358
	2	roof	3	x	0.005
	2	roof (PVC)	1		0.299
	2	roof (PVC)	1	x	0.008
	2	roof (PVC)	2		0.227
	2	roof (PVC)	2	x	0.008
	2	roof (PVC)	3		0.142
	2	roof (PVC)	3	x	0.003
	4	roof	1		2.396
	4	roof	1	x	0.117
	4	roof	2		1.480
	4	roof	2	x	0.005
	4	roof	3		0.706
	4	roof	3	x	0.008
	4	roof (PVC)	1		0.340
	4	roof (PVC)	1	x	0.010
	4	roof (PVC)	2		1.141
	4	roof (PVC)	2	x	0.005
	4	roof (PVC)	3		0.947
	4	roof (PVC)	3	x	0.010
	Synthetic Water 1	n/a	n/a		0.000
	Synthetic Water 1	n/a	n/a	x	0.000
	Synthetic Water 2	n/a	n/a		0.117
	Synthetic Water 2	n/a	n/a	x	0.000

Natural Rain Wall Runoff (Collection Event #1)

The wall runoff samples seem to indicate a high level of lead present, comparable or above the lead concentration values found in the roof runoff samples. However, definitive discussion of these results cannot take place due to the low number of samples taken. Plans are in progress to collect additional wall runoff samples using synthetic rain water similar to that used for the third collection event.

Natural Rain Roof Runoff (Collection Events #1 and #2)

Significant amounts of lead were found in the roof runoff samples. Generally, samples of the first flush of roof runoff showed higher levels of lead than the second and third samples afterwards, although departures from this pattern can be seen. Additional collections will help to ascertain whether later samples are significantly different than first flush samples, or whether natural variability in concentration is responsible for these departures. Below is a graphic representation of the results obtained from the natural rain roof runoff collection #2. A third sample was not taken from house number 4.
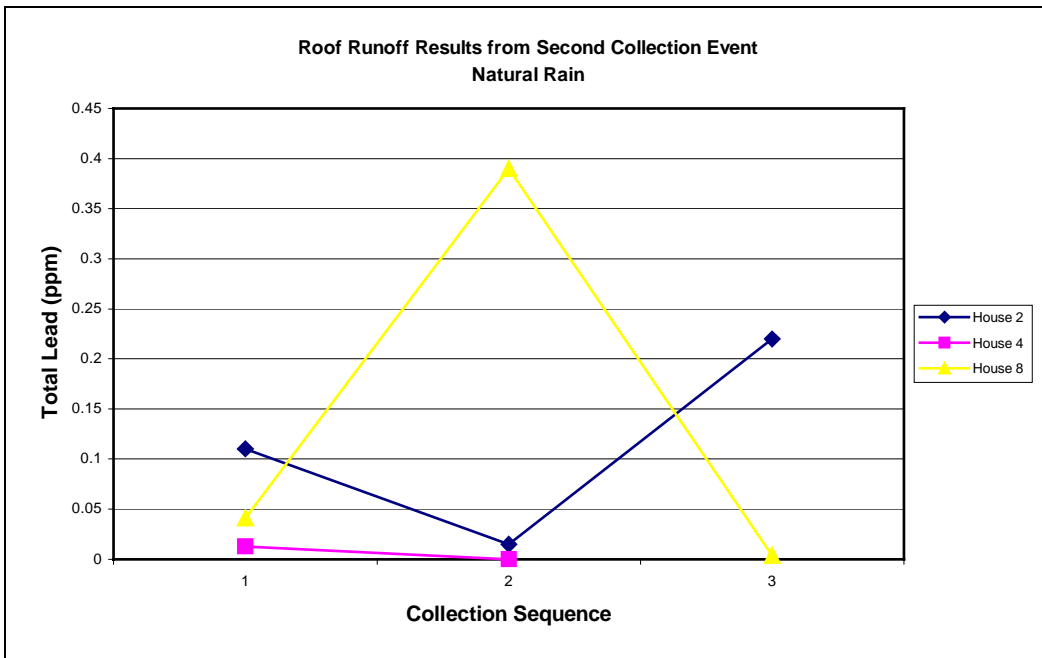
Results from the second collection event indicate that there is generally a very large decrease in the amount of lead found in filtered vs. unfiltered samples. The average decrease in the concentration after filtering was 89%. Thus, it appears that most of the lead present in the roof runoff is of particulate form.

Synthetic Rain Roof Runoff (Collection Event #3)

The samples gathered during the third collection event using synthetic rain yielded higher lead concentrations than from the two previous collection events using natural rain. The

greatest difference occurs at house number 2 for the first flush results. With the synthetic rain water, the results show 11.708 ppm of lead, whereas the natural rain water collected during the second collection event show a level of 0.112 ppm of lead in the first flush. The third collection indicates an average of 99% higher values of lead as compared to the first flush in the second collection event. This may be attributed to the chemical make-up of the artificial rain as compared to natural rain, to the long time period of dry weather prior to the third collection date, or contamination of the sample on the third collection date.   Additional sampling of both natural and synthetic rain events will help the investigator investigate these various hypotheses.

The samples collected with the artificial PVC gutters on the third collection event yielded an average of 46% lower levels of lead than those collected with the natural metal gutters from the same house. This indicates that a portion of the lead contamination may be attributed to the contributions from the metal gutters. Below is a graphic representation of the unfiltered lead levels from the samples gathered during the third collection event. Note that the PVC gutters consistently yielded lower lead levels than the natural metal gutters from the same house.


Roof Runoff Results from Third Collection Event
Synthetic Rain
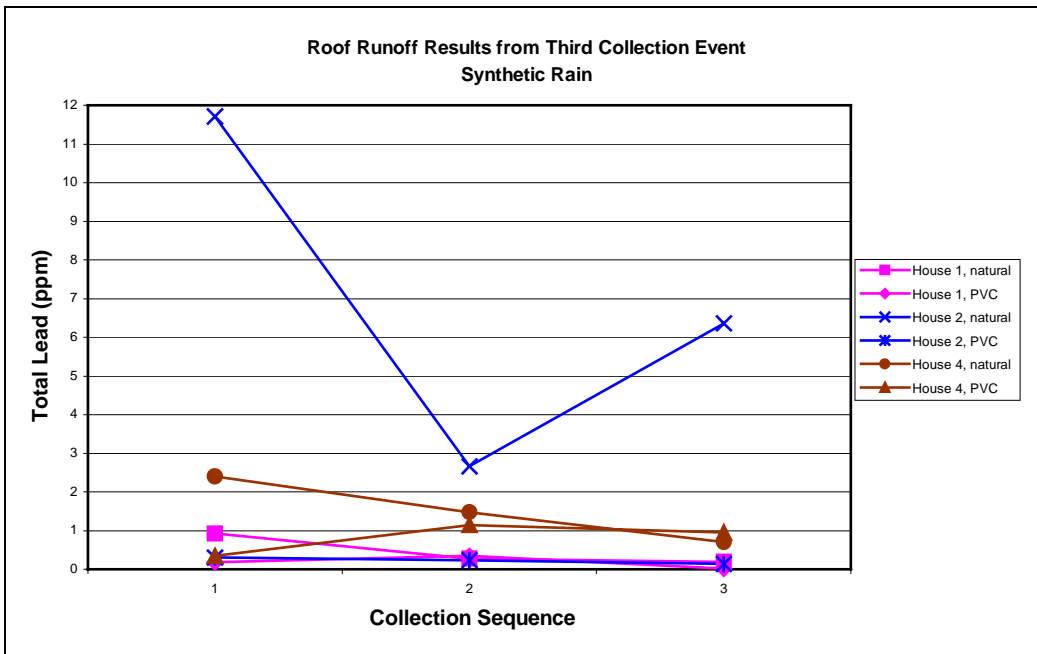
CONCLUSIONS

Rain runoff from rooftops and from the exterior walls of structures painted with lead-based paint is thought to be two sources of lead which may be contribute to non-point source loadings. This research has indicated that lead particulates in roof and wall runoff can be significant. Furthermore, these findings yield greater lead levels than those referenced in similar work done by other researchers. The first flush during the rain event generally gives the highest concentration of lead levels from the roof runoff samples, with decreasing levels for the second and third collections, respectively. However, some departures may be noted from this trend, which may be due to contaminated samples; to a change in the rain event, causing a greater intensity of rainfall, thus sloughing off more lead particles from the rooftop; or simply to natural variability. The lead found in these runoff samples is mostly in the particulate form, as the amount of lead detected in the filtered samples is generally miniscule.

The lead levels detected in the samples taken with synthetic rain water were generally higher than those samples collected during natural rain events. This may be attributed to the chemical make-up of the artificial rain as compared to natural rain, to the long time period of dry weather prior to the third collection date, or to contamination of samples. Furthermore, as discovered in the third collection event, in-place metal gutters increase the levels of lead found in runoff. The samples collected with the artificial PVC gutters yielded an average of 46% lower levels of lead than those collected with the natural metal gutters from the same house.

Although these results are preliminary, it can be seen that lead contamination from roof and wall runoff can be significant. Since the sample collection efforts in this project were somewhat hampered by the lack of rain in New Orleans over the past year, the principal investigator will continue collection and analysis of runoff samples through the spring and summer of 2001. These additional data will be used to evaluate the preliminary conclusions discussed here.

Figures 1-5
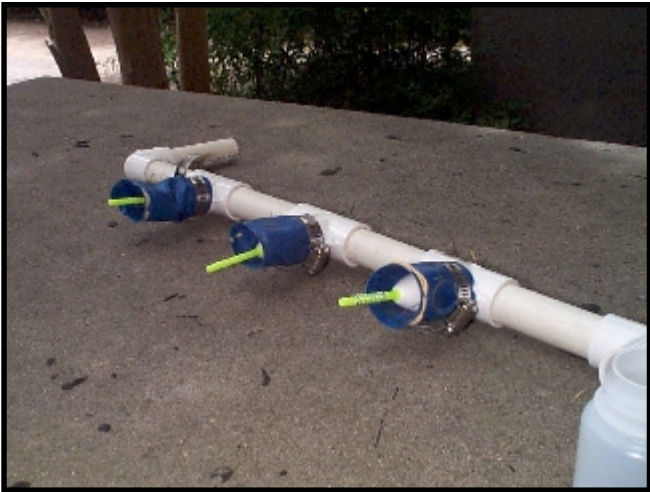
Figure 1. The PVC collection device and sample bottles which are placed at the base of the gutter for runoff collection.

Figure 2. Images of the artificial PVC gutter.

Figure 3. Putting the PVC gutter in place.

Figure 4. Pictures taken during

Figure 5. Water flowing through the vinyl tubing to the collection

REFERENCES

Cole, R.H., R.E. Frederick, R.P. Healy and R.G. Rolan, 1985. "Preliminary Findings of the Priority Pollutant Monitoring Project of the Nationwide Urban Runoff Program", *Journal of the Water Pollution Control Federation*, vol. 56, no. 7, pp. 898-908.

Davis, A.P. and Matthew Burns, 1999. "Evaluation of Lead Concentration in Runoff from Painted Structures", *Water Research*, vol. 33, no. 13, pp. 2949-2958.

Ellis, F.W. and R.L. Wycoff, 1981. "Cost-Effective Water Quality Planning for Urban Areas", *Journal of the Water Pollution Control Federation*, vol. 33, no. 13, pp. 246-258.

Flores-Rodriguez, J., A.L. Bussy and D.R. Thevenot, 1993. "Toxic metals in urban runoff: Physico-chemical mobility assessment using speciation schemes", *Water Science and Technology*, vol. 29, no. 1-2, pp. 83-93.

Good, J.C., 1993. "Roof runoff as a diffuse source of metals and aquatic toxicology in storm water", *Water Science Technology*, vol. 28, no. 3-5, pp. 291-297.

Kerri, K.D., J.A. Racine and R.B. Howell, 1985. "Forecasting Pollutant Loads from Highway Runoff", *Transportation Research Record*, no. 1017, pp. 39-46.

Louisiana Dept. of Environmental Quality, 1998. State of Louisiana Water Quality Management Plan, Water Quality Inventory Section 305(b) Report, Baton Rouge.

Martin, J.D., 1995. Effects of combined sewer overflows and urban runoff on the water quality of Fall Creek, Indianapolis, Indiana. U.S. Geological Survey, Water Resources Report 94-4066.

Mielke, H.W., C.R. Gonzales, M.K. Smith, and P.W. Mielke, 1999. "The Urban Environment and Children's Health: Soils as an Integrator of Lead, Zinc, and Cadmium in New Orleans, Louisiana, USA", *Environmental Research*, vol. 81, no. 2, pp. 117-129.

Ni, S., M. Shokouhian and A.P. Davis, 1995. Sources of lead, copper, cadmium, and zinc in urban runoff in Prince Georges County, Maryland. Final report to the Prince Georges County government.

The Times-Picayune 2 January 2001, sec. B.

The Times-Picayune 27 May 2001, sec. B.

Tsihrintizis, V.A. and R. Hamid, 1998. "Runoff quality prediction from small urban catchments using SWMMM", *Hydrological Processes*, vol. 12, no. 2, pp. 311-329.

U.S. Environmental Protection Agency, 1993. Results of the Nationwide Urban Runoff Program: Final Report. Water Planning Division, USEPA, Washington, D.C.

Whipple, W. Jr. and J.V. Hunter, 1981. Settleability of Urban Runoff Pollution", *Journal of the Water Pollution Control Federation*, vol. 53, no. 12, pp. 1726-1731.

Yaziz, M.I., H. Gunting, N. Sapari, and A.W. Ghazali, 1989. "Variations in Rainwater Quality from Roof Catchments". *Water Research*, vol. 23, no. 6, pp. 761-765.

Information Transfer Program

The information transfer activities of the Institute during the Fiscal Year 2000 consisted of participation in conferences, maintaining contact with several federal, state and local agencies, and making several presentations to the general public.

The Institute participated in several conferences. It was a co-host of the 2000 Annual Conference of Universities Council of Water Resources, held in New Orleans. It also made presentations at the Louisiana State Flood Plain Managers Association meeting, the National Hurricane Conference, the Louisiana Association of Levee Boards, and a Sea Grant meeting on coastal hazards. Several presentations were made to civic groups in the state, including the Southeastern Louisiana Economic Council, the I-10 Alliance, the Lake Pontchartrain Basin Foundation, and the New Orleans Regional Planning Commission. The Institute worked with several local and state governmental agencies including the Coastal Wetland Planning, Protection and Restoration Act task force, the Governor's Office of Coastal Activities, St. James Parish, Jefferson Parish, Orleans Parish, St Tammany Parish, the Amite River Basin Commission, the Louisiana Office of Emergency Preparedness, and the La. Department of Transportation and Development.

The Natural Systems Engineering Laboratory (NSEL) has for the last few years worked with state and parish emergency response agencies concerning hurricane flood protection. The laboratory provides realtime forecasts of the coastal flooding, based upon information provided by the National weather Service. This year a project called "Community Haven" was initiated. The concept of the community have is to protect a smaller area of a coastal community to a higher level of protection than can be provided for the community as a whole. It is being developed in more detail for the New Orleans Metropolitan Area. This concept has attracted considerable interest among the news media including several newspapers and TV stations in Baton Rouge and New Orleans. It has also been featured on CNN (Earth Matters), the Discovery Channel, Time Magazine, and ABC national news. The issue of hurricane flood protection was also presented to the Louisiana Congressional Delegation and to FEMA.

The Institute's staff has maintained emphasis on acquainting Louisiana's research community with the research funding opportunities through the U.S. Geological Survey Section 104 research program. Announcements for the 104 program were widely distributed (300+) to Louisiana college and universities and to research organizations throughout the state. In addition, public announcements were made at professional and faculty meetings to encourage wide participation in the program. Table 1 depicts this participation in response to the announcements.

Table 1. Louisiana's Participation in LWRRI Research Programs, Proposals Submitted

Year Section 104 Section 105 2000 12 3 Funded

The Director attended the annual National Institutes of Water Resources meetings in Washington, D. C., to discuss Institute and Program activities.

USGS Summer Intern Program

Student Support

Category	Section 104 Base Grant	Section 104 RCGP Award	NIWR-USGS Internship	Supplemental Awards	Total
Undergraduate	3	0	0	0	3
Masters	4	0	0	0	4
Ph.D.	2	0	0	0	2
Post-Doc.	1	0	0	0	1
Total	10	0	0	0	10

Notable Awards and Achievements

The Institute now has a program that has statewide and national impact and recognition. The Institute research and service program in hurricane flooding has been the subject of media coverage by several local newspapers, radio and TV segments. It has been covered by ABC national news (Peter Jennings), CNN - Earth Matters, and in a separate article in Time Magazine. Recent interviews have been held with CNN and with Scientific American. The Institute provides realtime forecasts of hurricane flooding to parish and state emergency managers to assist them in decision making. The Institute program in coastal restoration has produced results that have been used by several state and federal agencies involved with the Coastal Wetland Protection, Planning and Restoration Act program. The Secretary of the Louisiana Department of Natural Resources used Institute projections of future landloss in his presentation to Congress supporting the Conservation and Restoration Act (CARA). The Institute maintains contact with several researchers on the LSU campus and on university campuses statewide to foster cooperation in water resources research. The Institute has continued to maintain a strong externally funded research program supported by a variety of funding agencies and institutions. Recent funding has been obtained from the U. S. Army Corps of Engineers, The Louisiana University Marine Consortium, St. James and Jefferson Parishes, the National Aeronautics and Space Administration, the Lake Pontchartrain Basin Foundation, the Governor's Office of Coastal Activities, the Barataria/Terrebonne National Estuaries Program, and the Louisiana Department of Natural Resources.

Publications from Prior Projects

1. Books 1. Singh, P. and Singh, V. P., Snow and Glacier Hydrology. Kluwer Academic Publishers, 742 pp., 2000
2. Edited Books 1. Singh, V. P., Frevert, D. K.,and Meyer, S. P., editors, Mathematical Modeling of Large Watershed Hydrology. Water Resources Publications, Littleton Colorado, 2001.
3. Book Chapters 1. Singh, V. P., Bengtsson, L., and Westerstrom, G., 2000, Kinematic Wave Modelling of Saturated Basal Flow in a Snowpack. pp. 283-294 in High Resolution Flow Modeling in Hydrology and Geomorphology, edited by P. D. Bates and S. N. Lane, John Wiley & Sons, New York, 2000.
4. 2. Singh, V. P., Wang, G.-T., and Adrian, D. D., Flood Routing Based on Diffusion Wave Equation Using Mixing Cell Method. pp. 167-180 in High Resolution Flow Modeling in Hydrology and Geomorphology, edited by P. D. Bates and S. N. Lane, John Wiley & Sons, New

York, 2000.

5. 3. Singh, V. P., Frevert, D. K. and Meyer, S. P., Mathematical Modeling of Watershed Hydrology. Chapter 1 in Mathematical Models of Large Watershed Hydrology, edited by V. P. Singh, D. K. Frevert and S. P. Meyer, Water Resources Publications, Littleton, Colorado, in press, 2001.

6. 4. Singh, V. P., Frevert, D. K. and Meyer, S. P., Mathematical Modeling of Watershed Hydrology. Chapter 1 in Mathematical Models of Small Watershed Hydrology and Applications, edited by V. P. Singh, D. K. Frevert and S. P. Meyer, Water Resources Publications, Littleton, Colorado, in press, 2001.

7. 5. Mishra, S. K. and Singh, V. P., SCS-CN_Based Hydrologic Simulation Package. Chapter 13 in Mathematical Models of Small Watershed Hydrology and Applications, edited by V. P. Singh, D. K. Frevert and S. P. Meyer, Water Resources Publications, Littleton, Colorado, in press, 2001.

8. 6. Ojha, C. S. P. and Singh, V. P., Models of Water Balance in a Small Watershed. Chapter 14 in Mathematical Models of Small Watershed Hydrology and Applications, edited by V. P. Singh, D. K. Frevert and S. P. Meyer, Water Resources Publications, Littleton, Colorado, in press, 2001.

9. 7. Ojha, C. S. P. and Singh, V. P., ANN Modeling in Watershed Hydrology. Chapter 3 in Mathematical Models of Large Watershed Hydrology, edited by V. P. Singh, D. K. Frevert and S. P. Meyer, Water Resources Publications, Littleton, Colorado, in press, 2001.

10. 8. Singh, V. P., Statistical Analyses Design. in Encyploedia of Life Support Systems, edited by A. Sydom, EOLSS Publishers Co., Ltd., Oxford, U. K., 2001.

11. 9. Ojha, C. S. P. and Singh, V. P., Storm Water Drainage and Effluent Disposal. in Encyploedia of Life Support Systems, edited by A. Sydom, EOLSS Publishers Co., Ltd., Oxford, U. K., 2001.

12. 10. Harmancioglu, N. B. and Singh, V. P., Data Accuracy and Validation. in Encyploedia of Life Support Systems, edited by A. Sydom, EOLSS Publishers Co., Ltd., Oxford, U. K., 2001.

13. 11. Singh, V. P., The Entropy Theory as a Decision Making Tool in Environmental and Water Resources. in Entropy Measures, maximum Entropy and Emerging Applications, edited by Karmeshu, Springer-Verlag, Bonn, Germany.

14. 12. Singh, V.P., Ecological Hydrology. in: Hydrology in Environmental Management, edited by J.S. Rawat, Shree Almora Book Depot, Almora, India, in press, 2001.

15. Articles in Refereed Journals 1. Xu, C.-Y. And Singh, V. P., Evaluation and Generalization of Radiation-Based Methods for calculating evaporation. Hydrological Processes, Vol. 14, No. 2, pp. 339-351, 2000.

16. 2. Moramarco, T. and Singh, V. P., A Practical Method for Analysis of River Waves and for Kinematic Wave Routing in Natural Channel Networks. Hydrological Processes, Vol. 14, pp. 51-62, 2000

17. 3. Singh, V. P., The Entropy Theory as Tool for Modeling and Decision Making in Environmental and Water Resources. Water SA, Vol. 26, No. 1, pp. 1-11, 2000.

18. 4. Ozkul, S., Harmancioglu, N.B. and Singh, V.P., Entropy-Based Assessment of Water Quality Monitoring Networks in Space/Time Dimensions. Journal of Hydrologic Engineering, ASCE, Vol. 5, No. 1, pp. 90-100, 2000.

19. 5. Bobba, A. G., Singh, V.P. and Bengtsson, L., Application of Environmental Mdels to Different Hydrological Systems. Ecological Modelling, Vol. 125, pp. 15-49, 2000.

20. 6. Westerstrom, G. and Singh, V. P., An Investigation of Snowmelt Runoff on Experimental Plots in Lulea, Sweden. Hydrological Processes, Vol.14, pp.1869-1885, 2000.

21. 7. Bobba, A. G., Singh, V.P. , Berndtssson, R. and Bengtsson, L., Numerical Simulation of Saltwater Intrusion into Laccadive Island Aquifers due to Climate Change. Indian Journal of Geophysics, Vol.55, pp. 589-612, 2000.

22. 8. Moramarco, T. and Singh, V. P., A Simple Method for Relating Local Stage and Remote Discharge. Journal of Hydrologic Engineering, ASCE, Vol. 6, No.1, pp.78-81, 2001.

23. 9. Singh, V. P., Water Power. The World Book Encyclopedia, pp., Chicago, Illinois, 2000.

24. 10. Singh, V. P., Kinematic Wave Modeling in Water Resources: A Historical Perspective. Hydrological Processes, Vol. 15, pp. 671-706, 2001.

25. 11. Bengtsson, L. and Singh, V. P., Model sophistication in relation to scales in Snowmelt Runoff Modeling. Nordic Hydrology, Vol., pp., 2001.

26. 12. Xu, C. Y. and Singh, Evaluation and Generalization of Temperature-Based Methods for Calculating Evaporation. Hydrological Processes, Vol., pp., in press, 2001.

27. 13 Mishra, S. K. and Singh, V. P., On the Seddon Speed Formula. Hydrological Sciences Journal, Vol., No., pp., in press, 2001.

28. 14. Mishra, S. K. and Singh, V. P., Reply to Discussions on "Another Look at SCS-CN Method." Journal of Hydrologic Engineering, ASCE, Vol., No., pp., in press, 2001.

29. 15. Mishra, S. K. and Singh, V. P., Hysteresis-Based Flood Wave Analysis Using the Concept of Strain. Hydrological Processes, Vol. Pp., in press, 2001.

30. 16. Melone, F., Corradini and Singh, V. P., A Comparative Analysis of the Formulations for basin Lag Prediction in Ungaged Basins. Hydrological Processes, Vol., pp., in press, 2001.

31. 17. Kawachi, T., Maruyama, T. and Singh, V. P., Rainfall Entropy for Delineation of Water Resources Zones in Japan. Journal of Hydrology, Vol., pp., inn press, 2001.

32. 18. Tsai, C. N., Adrian, D. D. and Singh, V. P., Finite Fourier Probability Distribution and Applications. Journal of Hydrologic Engineering, ASCE, Vol., No., pp. in press, 2001.

33. 19. Strupczewski, W. G., Singh, V. P. and Feluch, W., Non-stationary Approach to At-site Flood Frequency Modeling: 1. Maximum Likelihood Estimation. Journal of Hydrology, Vol., pp., in press, 2001.

34. 20. Strupczewski, W. G., Singh, V. P. and Mitosek, H. T., Non-stationary Approach to At-site Flood Frequency Modeling: 3. Flood Analysis of Polish Rivers. Journal of Hydrology, Vol., pp., in press, 2001.

35. 21. Singh, V. P., Is Hydrology Kinematic? Hydrological Processes, Vol., pp., in press, 2001.

36. Conference Proceedings 1. Mishra, S. K., Jain, S. K., Sharma, M. K. and Singh, V. P., Derivation of CN for Existing and Modeified SCSW-CN Methods. Proceedings, Regional Seminar on Conflict Management of International River basins, held December 7-8, 1999, in Dhaka, Bangladesh.

37. 2. Singh, V. P., Frevert, D. K., Trevino, M. A., Meyer, S. P. and Rieker, J. D., The Hydrologic Modeling Inventory - A Cooperative Research Effort. Proceedings, ASCE National Symposium on Watershed Management, Fort Collins, Colorado, in press, 2000.

38. 3. Singh, V. P., Hierarchy of Hydraulic Geometry Relations. Proceedings, Eight International Symposium on Stochastic Hydraulics, Beijing China, in press, 2000.

39. 4. Deng, Z. Q. and Singh, V. P., Fractal and Chaotic Characteristics of Alluvial Rivers. In Stochastic Hydraulics, edited by Z. Y. Wang and S. X. Hu, Balkema, Rotterdam, pp. 117-123, 2000.

40. 5. Tommaso, M. and Singh, V. P., Unsteady Overland Flow: Effects of the Boundary Conditions. Proceedings of the IASTED International Conference on Modeling and Simulation, pp. 1- 8, Philadelphia, May 15-17, 2001.